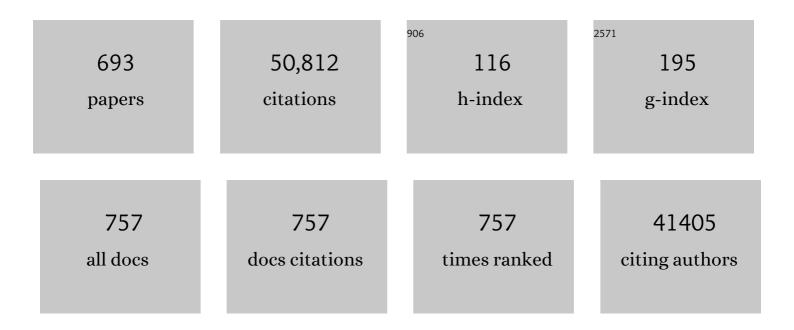
## Stefan Kaskel

List of Publications by Year in descending order

Source: https://exaly.com/author-pdf/9370294/publications.pdf Version: 2024-02-01



STEEAN KASKEI

#	Article	IF	CITATIONS
1	KOH activation of carbon-based materials for energy storage. Journal of Materials Chemistry, 2012, 22, 23710.	6.7	2,127
2	Flexible metal–organic frameworks. Chemical Society Reviews, 2014, 43, 6062-6096.	38.1	1,741
3	MOF-derived electrocatalysts for oxygen reduction, oxygen evolution and hydrogen evolution reactions. Chemical Society Reviews, 2020, 49, 1414-1448.	38.1	1,128
4	Improved synthesis, thermal stability and catalytic properties of the metal-organic framework compound Cu3(BTC)2. Microporous and Mesoporous Materials, 2004, 73, 81-88.	4.4	977
5	Characterization of metal-organic frameworks by water adsorption. Microporous and Mesoporous Materials, 2009, 120, 325-330.	4.4	938
6	Understanding activity and selectivity of metal-nitrogen-doped carbon catalysts for electrochemical reduction of CO2. Nature Communications, 2017, 8, 944.	12.8	890
7	Functional inorganic nanofillers for transparent polymers. Chemical Society Reviews, 2007, 36, 1454.	38.1	557
8	A pressure-amplifying framework material with negative gas adsorption transitions. Nature, 2016, 532, 348-352.	27.8	490
9	Catalytic properties of MIL-101. Chemical Communications, 2008, , 4192.	4.1	480
10	Selective Binding of O <sub>2</sub> over N <sub>2</sub> in a Redox–Active Metal–Organic Framework with Open Iron(II) Coordination Sites. Journal of the American Chemical Society, 2011, 133, 14814-14822.	13.7	470
11	Direct prediction of the desalination performance of porous carbon electrodes for capacitive deionization. Energy and Environmental Science, 2013, 6, 3700.	30.8	461
12	Solution infiltration of palladium into MOF-5: synthesis, physisorption and catalytic properties. Journal of Materials Chemistry, 2007, 17, 3827.	6.7	450
13	High-Rate Electrochemical Capacitors Based on Ordered Mesoporous Silicon Carbide-Derived Carbon. ACS Nano, 2010, 4, 1337-1344.	14.6	447
14	Graphene Quantum Dotsâ€Capped Magnetic Mesoporous Silica Nanoparticles as a Multifunctional Platform for Controlled Drug Delivery, Magnetic Hyperthermia, and Photothermal Therapy. Small, 2017, 13, 1602225.	10.0	379
15	Rattleâ€Type Fe <sub>3</sub> O <sub>4</sub> @SiO <sub>2</sub> Hollow Mesoporous Spheres as Carriers for Drug Delivery. Small, 2010, 6, 471-478.	10.0	361
16	Carbon Materials for Lithium Sulfur Batteries—Ten Critical Questions. Chemistry - A European Journal, 2016, 22, 7324-7351.	3.3	353
17	Comprehensive study of carbon dioxide adsorption in the metal–organic frameworks M <sub>2</sub> (dobdc) (M = Mg, Mn, Fe, Co, Ni, Cu, Zn). Chemical Science, 2014, 5, 4569-4581.	7.4	342
18	Aromatic porous-honeycomb electrodes for a sodium-organic energy storage device. Nature Communications, 2013, 4, 1485.	12.8	327

#	Article	IF	CITATIONS
19	Controlling Dendrite Growth in Solid-State Electrolytes. ACS Energy Letters, 2020, 5, 833-843.	17.4	322
20	A Mesoporous Metal–Organic Framework. Angewandte Chemie - International Edition, 2009, 48, 9954-9957.	13.8	317
21	Synergistic electroreduction of carbon dioxide to carbon monoxide on bimetallic layered conjugated metal-organic frameworks. Nature Communications, 2020, 11, 1409.	12.8	317
22	ZnO Hard Templating for Synthesis of Hierarchical Porous Carbons with Tailored Porosity and High Performance in Lithium‧ulfur Battery. Advanced Functional Materials, 2015, 25, 287-297.	14.9	315
23	Nanosized BiOX (X = Cl, Br, I) Particles Synthesized in Reverse Microemulsions. Chemistry of Materials, 2007, 19, 366-373.	6.7	312
24	Porphyrinâ€Based Metal–Organic Frameworks for Biomedical Applications. Angewandte Chemie - International Edition, 2021, 60, 5010-5035.	13.8	311
25	In-Situ Raman Investigation of Polysulfide Formation in Li-S Cells. Journal of the Electrochemical Society, 2013, 160, A1205-A1214.	2.9	305
26	New highly porous aluminium based metal-organic frameworks: Al(OH)(ndc) (ndc=2,6-naphthalene) Tj ETQq0 0 Materials, 2009, 122, 93-98.	0 rgBT /Ov 4.4	verlock 10 Tf 5 298
27	Sulfurâ€Infiltrated Micro―and Mesoporous Silicon Carbideâ€Derived Carbon Cathode for Highâ€Performance Lithium Sulfur Batteries. Advanced Materials, 2013, 25, 4573-4579.	21.0	296
28	Challenges and Key Parameters of Lithium-Sulfur Batteries on Pouch Cell Level. Joule, 2020, 4, 539-554.	24.0	288
29	Improved Hydrogen Storage Properties of Ti-Doped Sodium Alanate Using Titanium Nanoparticles as Doping Agents. Advanced Materials, 2003, 15, 1012-1015.	21.0	283
30	Hierarchical Micro―and Mesoporous Carbideâ€Derived Carbon as a Highâ€Performance Electrode Material in Supercapacitors. Small, 2011, 7, 1108-1117.	10.0	283
31	Balancing Mechanical Stability and Ultrahigh Porosity in Crystalline Framework Materials. Angewandte Chemie - International Edition, 2018, 57, 13780-13783.	13.8	283
32	High capacity vertical aligned carbon nanotube/sulfur composite cathodes for lithium–sulfur batteries. Chemical Communications, 2012, 48, 4097.	4.1	282
33	Tailoring porosity in carbon materials for supercapacitor applications. Materials Horizons, 2014, 1, 157-168.	12.2	278
34	A Phthalocyanineâ€Based Layered Twoâ€Dimensional Conjugated Metal–Organic Framework as a Highly Efficient Electrocatalyst for the Oxygen Reduction Reaction. Angewandte Chemie - International Edition, 2019, 58, 10677-10682.	13.8	278
35	Hydrogels and Aerogels from Noble Metal Nanoparticles. Angewandte Chemie - International Edition, 2009, 48, 9731-9734.	13.8	271
36	Capture of Nerve Agents and Mustard Gas Analogues by Hydrophobic Robust MOF-5 Type Metal–Organic Frameworks. Journal of the American Chemical Society, 2011, 133, 11888-11891.	13.7	270

#	Article	IF	CITATIONS
37	Neutron Powder Diffraction Study of D2Sorption in Cu3(1,3,5-benzenetricarboxylate)2. Journal of the American Chemical Society, 2006, 128, 15578-15579.	13.7	266
38	Reduced polysulfide shuttle in lithium–sulfur batteries using Nafion-based separators. Journal of Power Sources, 2014, 251, 417-422.	7.8	265
39	Highly Hydrophobic Isoreticular Porous Metal–Organic Frameworks for the Capture of Harmful Volatile Organic Compounds. Angewandte Chemie - International Edition, 2013, 52, 8290-8294.	13.8	264
40	Zr- and Hf-Based Metal–Organic Frameworks: Tracking Down the Polymorphism. Crystal Growth and Design, 2013, 13, 1231-1237.	3.0	262
41	Adsorption and Detection of Hazardous Trace Gases by Metal–Organic Frameworks. Advanced Materials, 2018, 30, e1704679.	21.0	261
42	Negative Thermal Expansion in the Metal–Organic Framework Material Cu <sub>3</sub> (1,3,5â€benzenetricarboxylate) <sub>2</sub> . Angewandte Chemie - International Edition, 2008, 47, 8929-8932.	13.8	251
43	Metal–organic framework (MOF) aerogels with high micro- and macroporosity. Chemical Communications, 2009, , 6056.	4.1	248
44	Bimetallic Aerogels: Highâ€Performance Electrocatalysts for the Oxygen Reduction Reaction. Angewandte Chemie - International Edition, 2013, 52, 9849-9852.	13.8	246
45	An Efficient Route to Rattle-Type Fe3O4@SiO2 Hollow Mesoporous Spheres Using Colloidal Carbon Spheres Templates. Chemistry of Materials, 2009, 21, 2547-2553.	6.7	235
46	Proliferation, differentiation and gene expression of osteoblasts in boron-containing associated with dexamethasone deliver from mesoporous bioactive glass scaffolds. Biomaterials, 2011, 32, 7068-7078.	11.4	234
47	Topochemical conversion of an imine- into a thiazole-linked covalent organic framework enabling realÂstructure analysis. Nature Communications, 2018, 9, 2600.	12.8	232
48	Metal–Organic Frameworks with Exceptionally High Methane Uptake: Where and How is Methane Stored?. Chemistry - A European Journal, 2010, 16, 5205-5214.	3.3	227
49	Folate-Conjugated Fe <sub>3</sub> O <sub>4</sub> @SiO <sub>2</sub> Hollow Mesoporous Spheres for Targeted Anticancer Drug Delivery. Journal of Physical Chemistry C, 2010, 114, 16382-16388.	3.1	225
50	High pressure methane adsorption in the metal-organic frameworks Cu3(btc)2, Zn2(bdc)2dabco, and Cr3F(H2O)2O(bdc)3. Microporous and Mesoporous Materials, 2008, 112, 108-115.	4.4	209
51	Crystallographic insights into (CH <sub>3</sub> NH <sub>3</sub> ) <sub>3</sub> (Bi <sub>2</sub> 1 <sub>9</sub> ): a new lead-free hybrid organic–inorganic material as a potential absorber for photovoltaics. Chemical Communications, 2016. 52, 3058-3060.	4.1	208
52	Fungi-based porous carbons for CO2 adsorption and separation. Journal of Materials Chemistry, 2012, 22, 13911.	6.7	204
53	Toward a molecular design of porous carbon materials. Materials Today, 2017, 20, 592-610.	14.2	202
54	Elucidating Negative Thermal Expansion in MOF-5. Journal of Physical Chemistry C, 2010, 114, 16181-16186.	3.1	199

#	Article	IF	CITATIONS
55	Element–organic frameworks with high permanent porosity. Chemical Communications, 2008, , 2462.	4.1	197
56	A highly porous metal–organic framework, constructed from a cuboctahedral super-molecular building block, with exceptionally high methane uptake. Chemical Communications, 2012, 48, 10841.	4.1	197
57	Tailoring of network dimensionality and porosity adjustment in Zr- and Hf-based MOFs. CrystEngComm, 2013, 15, 9572.	2.6	196
58	Nickel cobalt oxide hollow nanosponges as advanced electrocatalysts for the oxygen evolution reaction. Chemical Communications, 2015, 51, 7851-7854.	4.1	195
59	Highly porous nitrogen-doped polyimine-based carbons with adjustable microstructures for CO2 capture. Journal of Materials Chemistry A, 2013, 1, 10951.	10.3	189
60	In Situ Formation of Protective Coatings on Sulfur Cathodes in Lithium Batteries with LiFSIâ€Based Organic Electrolytes. Advanced Energy Materials, 2015, 5, 1401792.	19.5	189
61	Zr(iv) and Hf(iv) based metal–organic frameworks with reo-topology. Chemical Communications, 2012, 48, 8407.	4.1	187
62	Stretchable and Semitransparent Conductive Hybrid Hydrogels for Flexible Supercapacitors. ACS Nano, 2014, 8, 7138-7146.	14.6	186
63	Electronic Devices Using Open Framework Materials. Chemical Reviews, 2020, 120, 8581-8640.	47.7	185
64	Highâ€Performance Electrocatalysis on Palladium Aerogels. Angewandte Chemie - International Edition, 2012, 51, 5743-5747.	13.8	181
65	Improved Hydrogen Storage in the Metal-Organic Framework Cu3(BTC)2. Advanced Engineering Materials, 2006, 8, 293-296.	3.5	180
66	High-defect hydrophilic carbon cuboids anchored with Co/CoO nanoparticles as highly efficient and ultra-stable lithium-ion battery anodes. Journal of Materials Chemistry A, 2016, 4, 10166-10173.	10.3	179
67	A new metal–organic framework with ultra-high surface area. Chemical Communications, 2014, 50, 3450.	4.1	178
68	An Energy Storage Principle using Bipolar Porous Polymeric Frameworks. Angewandte Chemie - International Edition, 2012, 51, 7850-7854.	13.8	177
69	Variation in structure and Li+-ion migration in argyrodite-type Li6PS5X (X = Cl, Br, I) solid electrolytes. Journal of Solid State Electrochemistry, 2012, 16, 1807-1813.	2.5	176
70	Carbide-derived carbon aerogels with tunable pore structure as versatile electrode material in high power supercapacitors. Carbon, 2017, 113, 283-291.	10.3	171
71	Carbonâ€Based Anodes for Lithium Sulfur Full Cells with High Cycle Stability. Advanced Functional Materials, 2014, 24, 1284-1289.	14.9	168
72	Preparation, characterization and in vitro bioactivity of mesoporous bioactive glasses (MBGs) scaffolds for bone tissue engineering. Microporous and Mesoporous Materials, 2008, 112, 494-503.	4.4	166

#	Article	IF	CITATIONS
73	Gold Aerogels: Three-Dimensional Assembly of Nanoparticles and Their Use as Electrocatalytic Interfaces. ACS Nano, 2016, 10, 2559-2567.	14.6	165
74	Immobilization of <i>Trametes versicolor</i> Laccase on Magnetically Separable Mesoporous Silica Spheres. Chemistry of Materials, 2007, 19, 6408-6413.	6.7	162
75	Application of a chiral metal–organic framework in enantioselective separation. Chemical Communications, 2011, 47, 12089.	4.1	159
76	Promoting the sulfur redox kinetics by mixed organodiselenides in high-energy-density lithium–sulfur batteries. EScience, 2021, 1, 44-52.	41.6	159
77	Fine tuning of the metal–organic framework Cu3(BTC)2 HKUST-1 crystal size in the 100 nm to 5 micron range. Journal of Materials Chemistry, 2012, 22, 13742.	6.7	158
78	Imine-Linked Polymer-Derived Nitrogen-Doped Microporous Carbons with Excellent CO <sub>2</sub> Capture Properties. ACS Applied Materials & Interfaces, 2013, 5, 3160-3167.	8.0	158
79	High‣urfaceâ€Area Nanoporous Boron Carbon Nitrides for Hydrogen Storage. Advanced Functional Materials, 2010, 20, 1827-1833.	14.9	153
80	Expansion-tolerant architectures for stable cycling of ultrahigh-loading sulfur cathodes in lithium-sulfur batteries. Science Advances, 2020, 6, eaay2757.	10.3	152
81	Preparation of palladium supported on MOF-5 and its use as hydrogenation catalyst. Catalysis Communications, 2008, 9, 1286-1290.	3.3	149
82	A Highly Porous Metal–Organic Framework with Open Nickel Sites. Angewandte Chemie - International Edition, 2010, 49, 8489-8492.	13.8	149
83	Coke location in microporous and hierarchical ZSM-5 and the impact on the MTH reaction. Journal of Catalysis, 2013, 307, 238-245.	6.2	149
84	Comparison of the in vitro bioactivity and drug release property of mesoporous bioactive glasses (MBGs) and bioactive glasses (BGs) scaffolds. Microporous and Mesoporous Materials, 2009, 118, 176-182.	4.4	148
85	Multimetallic Aerogels by Template-Free Self-Assembly of Au, Ag, Pt, and Pd Nanoparticles. Chemistry of Materials, 2014, 26, 1074-1083.	6.7	148
86	Proline Functionalized UiO-67 and UiO-68 Type Metal–Organic Frameworks Showing Reversed Diastereoselectivity in Aldol Addition Reactions. Chemistry of Materials, 2016, 28, 2573-2580.	6.7	148
87	Ultrastable Surfaceâ€Dominated Pseudocapacitive Potassium Storage Enabled by Edgeâ€Enriched Nâ€Doped Porous Carbon Nanosheets. Angewandte Chemie - International Edition, 2020, 59, 19460-19467.	13.8	148
88	Micro―and Mesoporous Carbideâ€Derived Carbon–Selenium Cathodes for Highâ€Performance Lithium Selenium Batteries. Advanced Energy Materials, 2015, 5, 1400981.	19.5	144
89	Development and costs calculation of lithium–sulfur cells with high sulfur load and binder free electrodes. Journal of Power Sources, 2013, 224, 260-268.	7.8	142
90	Synthesis and Characterization of Transparent Luminescent ZnS:Mn/PMMA Nanocomposites. Chemistry of Materials, 2006, 18, 1068-1072.	6.7	141

#	Article	IF	CITATIONS
91	Thermal Exfoliation of Layered Metal–Organic Frameworks into Ultrahydrophilic Graphene Stacks and Their Applications in Li–S Batteries. Advanced Materials, 2017, 29, 1702829.	21.0	141
92	A cubic ordered, mesoporous carbide-derived carbon for gas and energy storage applications. Carbon, 2010, 48, 3987-3992.	10.3	140
93	Shuttle suppression in room temperature sodium–sulfur batteries using ion selective polymer membranes. Chemical Communications, 2014, 50, 3208.	4.1	140
94	Metal–Organic Framework/Graphene Quantum Dot Nanoparticles Used for Synergistic Chemo- and Photothermal Therapy. ACS Omega, 2017, 2, 1249-1258.	3.5	140
95	Monitoring adsorption-induced switching by 129Xe NMR spectroscopy in a new metal–organic framework Ni2(2,6-ndc)2(dabco). Physical Chemistry Chemical Physics, 2010, 12, 11778.	2.8	139
96	Chiral Metalâ€Organic Frameworks and Their Application in Asymmetric Catalysis and Stereoselective Separation. Chemie-Ingenieur-Technik, 2011, 83, 90-103.	0.8	139
97	Structural flexibility and intrinsic dynamics in the M2(2,6-ndc)2(dabco) (M = Ni, Cu, Co, Zn) metal–organic frameworks. Journal of Materials Chemistry, 2012, 22, 10303.	6.7	139
98	Lithium–sulfur batteries: Influence of C-rate, amount of electrolyte and sulfur loading on cycle performance. Journal of Power Sources, 2014, 268, 82-87.	7.8	139
99	High capacity micro-mesoporous carbon–sulfur nanocomposite cathodes with enhanced cycling stability prepared by a solvent-free procedure. Journal of Materials Chemistry A, 2013, 1, 9225.	10.3	138
100	Ultrahigh porosity in mesoporous MOFs: promises and limitations. Chemical Communications, 2014, 50, 7089.	4.1	138
101	Overcoming binder limitations of sheet-type solid-state cathodes using a solvent-free dry-film approach. Energy Storage Materials, 2019, 21, 390-398.	18.0	138
102	Heating and separation using nanomagnet-functionalized metal–organic frameworks. Chemical Communications, 2011, 47, 3075.	4.1	137
103	Alloy Anodes for Rechargeable Alkali-Metal Batteries: Progress and Challenge. , 2019, 1, 217-229.		135
104	Nonlinear Optical Switching in Regioregular Porphyrin Covalent Organic Frameworks. Angewandte Chemie - International Edition, 2019, 58, 6896-6900.	13.8	135
105	Kinetically Controlled Synthesis of PdNi Bimetallic Porous Nanostructures with Enhanced Electrocatalytic Activity. Small, 2015, 11, 1430-1434.	10.0	133
106	Synthesis and properties of the metal-organic framework Mo3(BTC)2 (TUDMOF-1). Journal of Materials Chemistry, 2006, 16, 2245.	6.7	132
107	Methane storage mechanism in the metal-organic framework Cu3(btc)2: An in situ neutron diffraction study. Microporous and Mesoporous Materials, 2010, 136, 50-58.	4.4	132
108	Carbideâ€Derived Carbon Monoliths with Hierarchical Pore Architectures. Angewandte Chemie - International Edition, 2012, 51, 7577-7580.	13.8	131

#	Article	IF	CITATIONS
109	Solid-State NMR Spectroscopy of Metal–Organic Framework Compounds (MOFs). Materials, 2012, 5, 2537-2572.	2.9	130
110	A Family of Chiral Metal–Organic Frameworks. Chemistry - A European Journal, 2011, 17, 2099-2106.	3.3	128
111	Route to a Family of Robust, Nonâ€interpenetrated Metal–Organic Frameworks with ptoâ€like Topology. Chemistry - A European Journal, 2011, 17, 13007-13016.	3.3	127
112	In Situ Synthesis of an Imidazolateâ€4â€amideâ€5â€imidate Ligand and Formation of a Microporous Zinc–Organic Framework with H <sub>2</sub> â€and CO <sub>2</sub> â€Storage Ability. Angewandte Chemie - International Edition, 2010, 49, 1258-1262.	13.8	126
113	Controlling the Growth of Palladium Aerogels with High-Performance toward Bioelectrocatalytic Oxidation of Glucose. Journal of the American Chemical Society, 2014, 136, 2727-2730.	13.7	124
114	Twin Polymerization at Spherical Hard Templates: An Approach to Sizeâ€Adjustable Carbon Hollow Spheres with Micro―or Mesoporous Shells. Angewandte Chemie - International Edition, 2013, 52, 6088-6091.	13.8	123
115	Carbon templated SAPO-34 with improved adsorption kinetics and catalytic performance in the MTO-reaction. Microporous and Mesoporous Materials, 2012, 164, 214-221.	4.4	122
116	A cubic coordination framework constructed from benzobistriazolate ligands and zinc ions having selective gas sorption properties. Dalton Transactions, 2009, , 6487.	3.3	120
117	Unusual Ultraâ€Hydrophilic, Porous Carbon Cuboids for Atmosphericâ€Water Capture. Angewandte Chemie - International Edition, 2015, 54, 1941-1945.	13.8	119
118	A semiconducting layered metal-organic framework magnet. Nature Communications, 2019, 10, 3260.	12.8	119
119	Ordered mesoporous carbide derived carbons for high pressure gas storage. Carbon, 2010, 48, 1707-1717.	10.3	115
120	High-Pressure in Situ <sup>129</sup> Xe NMR Spectroscopy and Computer Simulations of Breathing Transitions in the Metal–Organic Framework Ni <sub>2</sub> (2,6-ndc) <sub>2</sub> (dabco) (DUT-8(Ni)). Journal of the American Chemical Society, 2011, 133, 8681-8690.	13.7	113
121	3D Assembly of Semiconductor and Metal Nanocrystals: Hybrid CdTe/Au Structures with Controlled Content. Journal of the American Chemical Society, 2011, 133, 13413-13420.	13.7	112
122	MOF Processing by Electrospinning for Functional Textiles. Advanced Engineering Materials, 2011, 13, 356-360.	3.5	112
123	Metalâ€Organic Frameworks in Monolithic Structures. Journal of the American Ceramic Society, 2010, 93, 2476-2479.	3.8	110
124	Lithium–sulphur batteries – binder free carbon nanotubes electrode examined with various electrolytes. Journal of Power Sources, 2012, 213, 239-248.	7.8	109
125	Current status and future perspectives of lithium metal batteries. Journal of Power Sources, 2020, 480, 228803.	7.8	109
126	Enabling Highâ€Energy Solidâ€State Batteries with Stable Anode Interphase by the Use of Columnar Silicon Anodes. Advanced Energy Materials, 2020, 10, 2001320.	19.5	109

#	Article	IF	CITATIONS
127	Four-dimensional metal-organic frameworks. Nature Communications, 2020, 11, 2690.	12.8	109
128	Biological Chitin–MOF Composites with Hierarchical Pore Systems for Airâ€Filtration Applications. Angewandte Chemie - International Edition, 2015, 54, 12588-12591.	13.8	108
129	New element organic frameworks viaSuzuki coupling with high adsorption capacity for hydrophobic molecules. Soft Matter, 2010, 6, 3918.	2.7	106
130	Chemically activated fungi-based porous carbons for hydrogen storage. Carbon, 2014, 75, 372-380.	10.3	106
131	Unveiling reductant chemistry in fabricating noble metal aerogels for superior oxygen evolutionÂand ethanol oxidation. Nature Communications, 2020, 11, 1590.	12.8	106
132	Solvent-Induced Pore-Size Adjustment in the Metal-Organic Framework [Mg3(ndc)3(dmf)4] (ndc =) Tj ETQq0 0 C	) rgBT /Ov	erlock 10 Tf 5
133	Improved catalytic performance of hierarchical ZSM-5 synthesized by desilication with surfactants. Microporous and Mesoporous Materials, 2013, 165, 148-157.	4.4	105
134	Tetrazine functionalized zirconium MOF as an optical sensor for oxidizing gases. Chemical Communications, 2015, 51, 2280-2282.	4.1	105
135	Polymerization of w/o Microemulsions for the Preparation of Transparent SiO2/PMMA Nanocomposites. Langmuir, 2005, 21, 6048-6053.	3.5	104
136	Phthalocyanineâ€Based 2D Conjugated Metalâ€Organic Framework Nanosheets for Highâ€Performance Microâ€5upercapacitors. Advanced Functional Materials, 2020, 30, 2002664.	14.9	104
137	Neutron Diffraction and Neutron Vibrational Spectroscopy Studies of Hydrogen Adsorption in the Prussian Blue Analogue Cu3[Co(CN)6]2. Chemistry of Materials, 2006, 18, 3221-3224.	6.7	102
138	Intrinsic Shuttle Suppression in Lithium-Sulfur Batteries for Pouch Cell Application. Journal of the Electrochemical Society, 2017, 164, A3766-A3771.	2.9	101
139	Synthesis and characterisation of titanium nitride based nanoparticles. Journal of Materials Chemistry, 2003, 13, 1496.	6.7	100
140	Continuous microreactor synthesis of ZIF-8 with high space–time-yield and tunable particle size. Chemical Engineering Journal, 2016, 283, 971-977.	12.7	100

Chemical Engineering Journal, 2016, 283, 971-977. A new route for the preparation of mesoporous carbon materials with high performance in lithium–sulphur battery cathodes. Chemical Communications, 2013, 49, 5832. Structural transformation and high pressure methane adsorption of Co2(1,4-bdc)2dabco. 142 4.4 96 Microporous and Mesoporous Materials, 2008, 116, 653-657. Ordered Mesoporous Carbide Derived Carbons: Novel Materials for Catalysis and Adsorption. Journal 143 3.1 of Physical Chemistry C, 2009, 113, 7755-7761. Exceptional adsorption-induced cluster and network deformation in the flexible metal–organic 144 framework DUT-8(Ni) observed by in situ X-ray diffraction and EXAFS. Physical Chemistry Chemical 2.8 96 Physics, 2015, 17, 17471-17479.

#	Article	IF	CITATIONS
145	Hierarchical Carbideâ€Derived Carbon Foams with Advanced Mesostructure as a Versatile Electrochemical Energyâ€Storage Material. Advanced Energy Materials, 2014, 4, 1300645.	19.5	96
146	MOF@PolyHIPEs. Advanced Engineering Materials, 2008, 10, 1151-1155.	3.5	95
147	Magnetic SBA-15/poly(N-isopropylacrylamide) composite: Preparation, characterization and temperature-responsive drug release property. Microporous and Mesoporous Materials, 2009, 123, 107-112.	4.4	94
148	Hard Carbon Anodes and Novel Electrolytes for Longâ€Cycleâ€Life Room Temperature Sodiumâ€Sulfur Full Cell Batteries. Advanced Energy Materials, 2016, 6, 1502185.	19.5	94
149	Mechanism understanding for stripping electrochemistry of Li metal anode. SusMat, 2021, 1, 506-536.	14.9	93
150	Adsorptive capturing and storing greenhouse gases such as sulfur hexafluoride and carbon tetrafluoride using metal–organic frameworks. Microporous and Mesoporous Materials, 2012, 156, 115-120.	4.4	92
151	The effect of crystallite size on pressure amplification in switchable porous solids. Nature Communications, 2018, 9, 1573.	12.8	92
152	Metal–organic frameworks in Germany: From synthesis to function. Coordination Chemistry Reviews, 2019, 380, 378-418.	18.8	91
153	High surface area carbide-derived carbon fibers produced by electrospinning of polycarbosilane precursors. Carbon, 2010, 48, 403-407.	10.3	90
154	Interaction of electrolyte molecules with carbon materials of well-defined porosity: characterization by solid-state NMR spectroscopy. Physical Chemistry Chemical Physics, 2013, 15, 15177.	2.8	90
155	PECylated hollow mesoporous silica nanoparticles as potential drug delivery vehicles. Microporous and Mesoporous Materials, 2011, 141, 199-206.	4.4	89
156	Catalytic properties of high surface area titanium nitride materials. Journal of Molecular Catalysis A, 2004, 208, 291-298.	4.8	88
157	Crystal Growth of the Metal—Organic Framework Cu <sub>3</sub> (BTC) <sub>2</sub> on the Surface of Pulp Fibers. Advanced Engineering Materials, 2009, 11, 93-95.	3.5	86
158	N-Heterocyclic carbene containing element organic frameworks as heterogeneous organocatalysts. Chemical Communications, 2011, 47, 4814.	4.1	86
159	Dye Encapsulation Inside a New Mesoporous Metal–Organic Framework for Multifunctional Solvatochromicâ€Response Function. Chemistry - A European Journal, 2012, 18, 13299-13303.	3.3	86
160	A Mixed Ether Electrolyte for Lithium Metal Anode Protection in Working Lithium–Sulfur Batteries. Energy and Environmental Materials, 2020, 3, 160-165.	12.8	85
161	Transparent and luminescent YVO4 : Eu/polymer nanocomposites prepared by in situpolymerization. Journal of Materials Chemistry, 2007, 17, 758-765.	6.7	84
162	High surface area polyHIPEs with hierarchical pore system. Soft Matter, 2009, 5, 1055.	2.7	84

#	Article	IF	CITATIONS
163	A lithium–sulfur full cell with ultralong cycle life: influence of cathode structure and polysulfide additive. Journal of Materials Chemistry A, 2015, 3, 3808-3820.	10.3	84
164	Fabrication of nitrogen and sulfur co-doped hollow cellular carbon nanocapsules as efficient electrode materials for energy storage. Energy Storage Materials, 2018, 13, 72-79.	18.0	83
165	Binaphthalene-Based, Soluble Polyimides: The Limits of Intrinsic Microporosity. Macromolecules, 2009, 42, 8017-8020.	4.8	82
166	Integration of accessible secondary metal sites into MOFs for H <sub>2</sub> S removal. Inorganic Chemistry Frontiers, 2014, 1, 325-330.	6.0	81
167	Cationic microporous polymer networks by polymerisation of weakly coordinating cations with CO <sub>2</sub> -storage ability. Journal of Materials Chemistry A, 2014, 2, 11825-11829.	10.3	81
168	Self-Supporting Hierarchical Porous PtAg Alloy Nanotubular Aerogels as Highly Active and Durable Electrocatalysts. Chemistry of Materials, 2016, 28, 6477-6483.	6.7	81
169	Catalytic properties of pristine and defect-engineered Zr-MOF-808 metal organic frameworks. Catalysis Science and Technology, 2018, 8, 3610-3616.	4.1	81
170	Nitrogenâ€Doped Biomassâ€Derived Carbon Formed by Mechanochemical Synthesis for Lithium–Sulfur Batteries. ChemSusChem, 2019, 12, 310-319.	6.8	81
171	Studies on preventing Li dendrite formation in Li–S batteries by using pre-lithiated Si microwire anodes. Journal of Power Sources, 2014, 248, 1058-1066.	7.8	80
172	Nanocasting Hierarchical Carbide-Derived Carbons in Nanostructured Opal Assemblies for High-Performance Cathodes in Lithium–Sulfur Batteries. ACS Nano, 2014, 8, 12130-12140.	14.6	79
173	SiC/MCM-48 and SiC/SBA-15 Nanocomposite Materials. Chemistry of Materials, 2004, 16, 2869-2880.	6.7	78
174	Hydrogen adsorption in the metal–organic frameworks Fe2(dobdc) and Fe2(O2)(dobdc). Dalton Transactions, 2012, 41, 4180.	3.3	78
175	Preparation and application of cellular and nanoporous carbides. Chemical Society Reviews, 2012, 41, 5053.	38.1	78
176	Sulfated Zirconia Nanoparticles Synthesized in Reverse Microemulsions:Â Preparation and Catalytic Properties. Langmuir, 2002, 18, 7428-7435.	3.5	77
177	Nanoporous copolymer networks through multiple Friedel–Crafts-alkylation—studies on hydrogen and methane storage. Journal of Materials Chemistry, 2011, 21, 2131-2135.	6.7	76
178	The Importance of Pore Size and Surface Polarity for Polysulfide Adsorption in Lithium Sulfur Batteries. Advanced Materials Interfaces, 2016, 3, 1600508.	3.7	76
179	Chiral Functionalization of a Zirconium Metal–Organic Framework (DUT-67) as a Heterogeneous Catalyst in Asymmetric Michael Addition Reaction. Inorganic Chemistry, 2018, 57, 1483-1489.	4.0	76
180	Enhancing performance of Li–S cells using a Li–Al alloy anode coating. Electrochemistry Communications, 2013, 36, 38-41.	4.7	75

#	Article	IF	CITATIONS
181	Intrinsically Microporous Poly(imide)s: Structureâ d'Porosity Relationship Studied by Gas Sorption and X-ray Scattering. Macromolecules, 2011, 44, 2025-2033.	4.8	74
182	Flexible and Hydrophobic Zn-Based Metal–Organic Framework. Inorganic Chemistry, 2011, 50, 8367-8374.	4.0	74
183	Conformation-Controlled Sorption Properties and Breathing of the Aliphatic Al-MOF [Al(OH)(CDC)]. Inorganic Chemistry, 2014, 53, 4610-4620.	4.0	74
184	Pt-Ni Aerogels as Unsupported Electrocatalysts for the Oxygen Reduction Reaction. Journal of the Electrochemical Society, 2016, 163, F998-F1003.	2.9	74
185	Proline Functionalization of the Mesoporous Metalâ~'Organic Framework DUT-32. Inorganic Chemistry, 2015, 54, 1003-1009.	4.0	73
186	Towards general network architecture design criteria for negative gas adsorption transitions in ultraporous frameworks. Nature Communications, 2019, 10, 3632.	12.8	73
187	Unraveling Structure and Dynamics in Porous Frameworks via Advanced In Situ Characterization Techniques. Advanced Functional Materials, 2020, 30, 1907847.	14.9	73
188	2D framework materials for energy applications. Chemical Science, 2021, 12, 1600-1619.	7.4	73
189	Three-Dimensional Porous Cd(II) Coordination Polymer with Large One-Dimensional Hexagonal Channels: High Pressure CH4and H2Adsorption Studies. Inorganic Chemistry, 2011, 50, 539-544.	4.0	72
190	A Stimuliâ€Responsive Zirconium Metal–Organic Framework Based on Supermolecular Design. Angewandte Chemie - International Edition, 2017, 56, 10676-10680.	13.8	72
191	Ordered mesoporous silicon carbide (OM-SiC) via polymer precursor nanocasting. Chemical Communications, 2006, , 2469.	4.1	71
192	Porous Dithiine-Linked Covalent Organic Framework as a Dynamic Platform for Covalent Polysulfide Anchoring in Lithium–Sulfur Battery Cathodes. Journal of the American Chemical Society, 2022, 144, 9101-9112.	13.7	71
193	High-throughput screening: speeding up porous materials discovery. Chemical Communications, 2011, 47, 5151.	4.1	69
194	High Area Capacity Lithium-Sulfur Full-cell Battery with Prelitiathed Silicon Nanowire-Carbon Anodes for Long Cycling Stability. Scientific Reports, 2016, 6, 27982.	3.3	69
195	Glassy Metal–Organicâ€Frameworkâ€Based Quasiâ€Solidâ€State Electrolyte for Highâ€Performance Lithiumâ€Metal Batteries. Advanced Functional Materials, 2021, 31, 2104300.	14.9	69
196	Porous Silicon Nitride as a Superbase Catalyst. Journal of Catalysis, 2001, 201, 270-274.	6.2	68
197	Flexible and Transparent SWCNT Electrodes for Alternating Current Electroluminescence Devices. ACS Applied Materials & Interfaces, 2009, 1, 1640-1644.	8.0	68
198	Postsynthetic Inner-Surface Functionalization of the Highly Stable Zirconium-Based Metal–Organic Framework DUT-67. Inorganic Chemistry, 2016, 55, 7206-7213.	4.0	68

#	Article	IF	CITATIONS
199	Tailoring adsorption induced phase transitions in the pillared-layer type metal–organic framework DUT-8(Ni). Dalton Transactions, 2017, 46, 4685-4695.	3.3	68
200	Tolerance of Flexible MOFs toward Repeated Adsorption Stress. ACS Applied Materials & Interfaces, 2015, 7, 22292-22300.	8.0	67
201	On the mechanistic role of nitrogen-doped carbon cathodes in lithium-sulfur batteries with low electrolyte weight portion. Nano Energy, 2018, 54, 116-128.	16.0	67
202	High power supercap electrodes based on vertical aligned carbon nanotubes on aluminum. Journal of Power Sources, 2013, 227, 218-228.	7.8	66
203	Bipolar porous polymeric frameworks for low-cost, high-power, long-life all-organic energy storage devices. Journal of Power Sources, 2014, 245, 553-556.	7.8	66
204	Synthesis of highly electrochemically active Li <sub>2</sub> S nanoparticles for lithium–sulfur-batteries. Journal of Materials Chemistry A, 2015, 3, 16307-16312.	10.3	66
205	Pore-Size Engineering of Silicon Imido Nitride for Catalytic Applications. Angewandte Chemie - International Edition, 2001, 40, 4204-4207.	13.8	65
206	Gas Storage in a Partially Fluorinated Highly Stable Three-Dimensional Porous Metal–Organic Framework. Inorganic Chemistry, 2013, 52, 7358-7366.	4.0	65
207	Assembly of metal–organic polyhedra into highly porous frameworks for ethene delivery. Chemical Communications, 2015, 51, 1046-1049.	4.1	65
208	Nanocomposites with Structure Domains of 0.5 to 3â€nm by Polymerization of Silicon Spiro Compounds. Angewandte Chemie - International Edition, 2009, 48, 8254-8258.	13.8	63
209	Tuning the gate-opening pressure and particle size distribution of the switchable metal–organic framework DUT-8(Ni) by controlled nucleation in a micromixer. Dalton Transactions, 2017, 46, 14002-14011.	3.3	63
210	Thermal stability of high surface area silicon carbide materials. Journal of Solid State Chemistry, 2006, 179, 2281-2289.	2.9	61
211	Role of Surface Functional Groups in Ordered Mesoporous Carbide-Derived Carbon/Ionic Liquid Electrolyte Double-Layer Capacitor Interfaces. ACS Applied Materials & Interfaces, 2014, 6, 2922-2928.	8.0	61
212	MOF@SiO 2 core-shell composites as stationary phase in high performance liquid chromatography. Microporous and Mesoporous Materials, 2018, 263, 268-274.	4.4	61
213	Platinum-Catalyzed Template Removal for the in Situ Synthesis of MCM-41 Supported Catalysts. Chemistry of Materials, 2006, 18, 2663-2669.	6.7	60
214	A new route to porous monolithic organic frameworks via cyclotrimerization. Journal of Materials Chemistry, 2011, 21, 711-716.	6.7	60
215	Mixed Aerogels from Au and CdTe Nanoparticles. Advanced Functional Materials, 2013, 23, 1903-1911.	14.9	60
216	Perspective on Carbon Anode Materials for K <sup>+</sup> Storage: Balancing the Intercalation ontrolled and Surfaceâ€Driven Behavior. Advanced Energy Materials, 2021, 11, 2100856.	19.5	60

#	Article	IF	CITATIONS
217	Pore size engineering of mesoporous silicon nitride materials. Physical Chemistry Chemical Physics, 2002, 4, 1675-1681.	2.8	58
218	In situ monitoring of structural changes during the adsorption on flexible porous coordination polymers by X-ray powder diffraction: Instrumentation and experimental results. Microporous and Mesoporous Materials, 2014, 188, 190-195.	4.4	58
219	BaHfO <sub>3</sub> artificial pinning centres in TFA-MOD-derived YBCO and GdBCO thin films. Superconductor Science and Technology, 2015, 28, 114002.	3.5	58
220	A Phthalocyanineâ€Based Layered Twoâ€Dimensional Conjugated Metal–Organic Framework as a Highly Efficient Electrocatalyst for the Oxygen Reduction Reaction. Angewandte Chemie, 2019, 131, 10787-10792.	2.0	58
221	Black BiVO <sub>4</sub> : size tailored synthesis, rich oxygen vacancies, and sodium storage performance. Journal of Materials Chemistry A, 2020, 8, 1636-1645.	10.3	58
222	3D Ni and Co redox-active metal–organic frameworks based on ferrocenyl diphosphinate and 4,4′-bipyridine ligands as efficient electrocatalysts for the hydrogen evolution reaction. Dalton Transactions, 2020, 49, 2794-2802.	3.3	58
223	Recent Progress and Emerging Application Areas for Lithium–Sulfur Battery Technology. Energy Technology, 2021, 9, 2000694.	3.8	58
224	Synthesis of Magnetically Separable Porous Carbon Microspheres and Their Adsorption Properties of Phenol and Nitrobenzene from Aqueous Solution. Journal of Physical Chemistry C, 2008, 112, 8623-8628.	3.1	57
225	A highly porous flexible Metal–Organic Framework with corundum topology. Chemical Communications, 2011, 47, 490-492.	4.1	57
226	Switchable Conductive MOF–Nanocarbon Composite Coatings as Threshold Sensing Architectures. ACS Applied Materials & Interfaces, 2017, 9, 43782-43789.	8.0	57
227	Polysulfide Shuttle Suppression by Electrolytes with Lowâ€Density for Highâ€Energy Lithium–Sulfur Batteries. Energy Technology, 2019, 7, 1900625.	3.8	57
228	Hydrophilic non-precious metal nitrogen-doped carbon electrocatalysts for enhanced efficiency in oxygen reduction reaction. Chemical Communications, 2015, 51, 17285-17288.	4.1	56
229	Three-dimensional interconnected nitrogen-doped mesoporous carbons as active electrode materials for application in electrocatalytic oxygen reduction and supercapacitors. Journal of Colloid and Interface Science, 2018, 527, 230-240.	9.4	56
230	Synthesis and catalytic properties of microemulsion-derived cerium oxide nanoparticles. Journal of Solid State Chemistry, 2008, 181, 1614-1620.	2.9	55
231	CFA-1: the first chiral metal–organic framework containing Kuratowski-type secondary building units. Dalton Transactions, 2013, 42, 10786.	3.3	55
232	A catalytically active porous coordination polymer based on a dinuclear rhodium paddle-wheel unit. Journal of Materials Chemistry A, 2014, 2, 144-148.	10.3	55
233	Precursor strategies for metallic nano- and micropatterns using soft lithography. Journal of Materials Chemistry C, 2015, 3, 2717-2731.	5.5	55
234	The influence of formation temperature on the solid electrolyte interphase of graphite in lithium ion batteries. Journal of Energy Chemistry, 2020, 49, 335-338.	12.9	55

#	Article	IF	CITATIONS
235	Micro- and mesoporous carbide-derived carbon prepared by a sacrificial template method in high performance lithium sulfur battery cathodes. Journal of Materials Chemistry A, 2014, 2, 17649-17654.	10.3	54
236	Crystal size <i>versus</i> paddle wheel deformability: selective gated adsorption transitions of the switchable metal–organic frameworks DUT-8(Co) and DUT-8(Ni). Journal of Materials Chemistry A, 2019, 7, 21459-21475.	10.3	54
237	Tunable Flexibility and Porosity of the Metal–Organic Framework DUT-49 through Postsynthetic Metal Exchange. Chemistry of Materials, 2020, 32, 889-896.	6.7	54
238	Tubular and Rodlike Ordered Mesoporous Silicon (Oxy)carbide Ceramics and their Structural Transformations. Chemistry of Materials, 2008, 20, 5421-5433.	6.7	53
239	Transition metal loaded silicon carbide-derived carbons with enhanced catalytic properties. Carbon, 2012, 50, 1861-1870.	10.3	53
240	Magnetic mesoporous bioactive glass scaffolds: preparation, physicochemistry and biological properties. Journal of Materials Chemistry B, 2013, 1, 1279.	5.8	53
241	Aqueous Solution Process for the Synthesis and Assembly of Nanostructured One-Dimensional α-MoO <sub>3</sub> Electrode Materials. Chemistry of Materials, 2013, 25, 2557-2563.	6.7	53
242	Nanostructure characterization of carbide-derived carbons by morphological analysis of transmission electron microscopy images combined with physisorption and Raman spectroscopy. Carbon, 2016, 105, 314-322.	10.3	53
243	Toward in-situ protected sulfur cathodes by using lithium bromide and pre-charge. Nano Energy, 2017, 40, 170-179.	16.0	53
244	Mechanochemical synthesis of multi-site electrocatalysts as bifunctional zinc–air battery electrodes. Journal of Materials Chemistry A, 2019, 7, 19355-19363.	10.3	53
245	Adaptive response of a metal–organic framework through reversible disorder–disorder transitions. Nature Chemistry, 2021, 13, 568-574.	13.6	53
246	Adsorption Contraction Mechanics: Understanding Breathing Energetics in Isoreticular Metal–Organic Frameworks. Journal of Physical Chemistry C, 2018, 122, 19171-19179.	3.1	52
247	Selective Permeable Lithiumâ€lon Channels on Lithium Metal for Practical Lithium–Sulfur Pouch Cells. Angewandte Chemie - International Edition, 2021, 60, 18031-18036.	13.8	52
248	New Chiral and Flexible Metalâ^'Organic Framework with a Bifunctional Spiro Linker and Zn <sub>4</sub> O-Nodes. Inorganic Chemistry, 2010, 49, 4440-4446.	4.0	51
249	Nanoimprint lithography of nanoporous carbon materials for micro-supercapacitor architectures. Nanoscale, 2018, 10, 10109-10115.	5.6	51
250	Insights into the water adsorption mechanism in the chemically stable zirconium-based MOF DUT-67 – a prospective material for adsorption-driven heat transformations. Journal of Materials Chemistry A, 2019, 7, 12681-12690.	10.3	51
251	Synthesis, characterization, and hydrogen storage capacities of hierarchical porous carbide derived carbon monolith. Journal of Materials Chemistry, 2012, 22, 23893.	6.7	50
252	Investigation of surface pre-treatments for the structural bonding of titanium. International Journal of Adhesion and Adhesives, 2012, 34, 46-54.	2.9	50

#	Article	IF	CITATIONS
253	Metal deposition by electroless plating on polydopamine functionalized micro- and nanoparticles. Journal of Colloid and Interface Science, 2013, 411, 187-193.	9.4	50
254	Carbon dioxide activated carbide-derived carbon monoliths as high performance adsorbents. Carbon, 2013, 56, 139-145.	10.3	50
255	Synthesis of Monoglycerides by Esterification of Oleic Acid with Glycerol in Heterogeneous Catalytic Process Using Tin–Organic Framework Catalyst. Catalysis Letters, 2013, 143, 356-363.	2.6	50
256	Selective Adsorption Properties of Cationic Metal–Organic Frameworks Based on Imidazolic Linker. Crystal Growth and Design, 2013, 13, 198-203.	3.0	49
257	Tailoring Pore Structure and Properties of Functionalized Porous Polymers by Cyclotrimerization. Macromolecules, 2014, 47, 4210-4216.	4.8	49
258	Postsynthetic Paddle-Wheel Cross-Linking and Functionalization of 1,3-Phenylenebis(azanetriyl)tetrabenzoate-Based MOFs. Chemistry of Materials, 2015, 27, 2460-2467.	6.7	49
259	Raman spectroscopy studies of the terahertz vibrational modes of a DUT-8 (Ni) metal–organic framework. Physical Chemistry Chemical Physics, 2017, 19, 32099-32104.	2.8	49
260	Magnetization relaxation in the single-ion magnet DySc <sub>2</sub> N@C <sub>80</sub> : quantum tunneling, magnetic dilution, and unconventional temperature dependence. Physical Chemistry Chemical Physics, 2018, 20, 11656-11672.	2.8	49
261	An Asymmetric Supercapacitor–Diode (CAPode) for Unidirectional Energy Storage. Angewandte Chemie - International Edition, 2019, 58, 13060-13065.	13.8	49
262	Characterization of the Metalâ^'Organic Framework Compound Cu3(benzene 1,3,5-tricarboxylate)2by Means of129Xe Nuclear Magnetic and Electron Paramagnetic Resonance Spectroscopy. Journal of Physical Chemistry B, 2006, 110, 20177-20181.	2.6	48
263	Oxide Foams for the Synthesis of High-Surface-Area Vanadium Nitride Catalysts. Advanced Materials, 2006, 18, 505-508.	21.0	48
264	Preparation, Microstructure, and Ferroelectric Properties of Bi <sub>3.25</sub> La <sub>0.75</sub> Ti <sub>3â^'<i>x</i></sub> M <sub><i>x</i></sub> O <sub>12</sub> (M) 1	[j හැQq0 (	) 04 <b>1</b> 88T /Ove
265	Platinum induced crosslinking of polycarbosilanes for the formation of highly porous CeO2/silicon oxycarbide catalysts. Journal of Materials Chemistry, 2009, 19, 1543.	6.7	48
266	Silicon oxycarbide-derived carbons from a polyphenylsilsequioxane precursor for supercapacitor applications. Microporous and Mesoporous Materials, 2014, 188, 140-148.	4.4	48
267	Rechargeable Al-ion batteries. EnergyChem, 2021, 3, 100049.	19.1	48
268	n-Butane adsorption on Cu3(btc)2 and MIL-101. Microporous and Mesoporous Materials, 2010, 129, 238-242.	4.4	47
269	Novel zeotype frameworks with soft cyclodiphosphazane linkers and soft Cu4X4 clusters as nodes. Chemical Communications, 2014, 50, 12273-12276.	4.1	47
270	Hopcalite nanoparticle catalysts with high water vapour stability for catalytic oxidation of carbon monoxide. Applied Catalysis B: Environmental, 2016, 184, 208-215.	20.2	47

#	Article	IF	CITATIONS
271	Ordered mesoporous carbide-derived carbons prepared by soft templating. Carbon, 2012, 50, 3987-3994.	10.3	46
272	Few-Layer Graphene Shells and Nonmagnetic Encapsulates: A Versatile and Nontoxic Carbon Nanomaterial. ACS Nano, 2013, 7, 10552-10562.	14.6	46
273	A stable lithiated silicon–chalcogen battery via synergetic chemical coupling between silicon and selenium. Nature Communications, 2017, 8, 13888.	12.8	46
274	Collective Breathing in an Eightfold Interpenetrated Metal–Organic Framework: From Mechanistic Understanding towards Threshold Sensing Architectures. Angewandte Chemie - International Edition, 2020, 59, 4491-4497.	13.8	46
275	The Role of Balancing Nanostructured Silicon Anodes and NMC Cathodes in Lithium-Ion Full-Cells with High Volumetric Energy Density. Journal of the Electrochemical Society, 2020, 167, 020516.	2.9	46
276	Spaceâ€Confined Formation of FePt Nanoparticles in Ordered Mesoporous Silica SBAâ€15. Advanced Materials, 2007, 19, 3021-3026.	21.0	45
277	Improved REBa2Cu3O7â^'x (RE = Y, Gd) structure and superconducting properties by addition of acetylacetone in TFA-MOD precursor solutions. Journal of Materials Chemistry A, 2014, 2, 4932.	10.3	45
278	Towards Chiral Microporous Soluble Polymers—Binaphthaleneâ€Based Polyimides. Macromolecular Rapid Communications, 2011, 32, 438-443.	3.9	44
279	Synthesis of Heteroâ€Polymer Functionalized Nanocarriers by Combining Surfaceâ€Initiated ATRP and RAFT Polymerization. Small, 2012, 8, 3579-3583.	10.0	44
280	Facile storage and release of white phosphorus and yellow arsenic. Nature Communications, 2018, 9, 361.	12.8	44
281	In Situ Observation of Gating Phenomena in the Flexible Porous Coordination Polymer Zn <sub>2</sub> (BPnDC) <sub>2</sub> (bpy) (SNU-9) in a Combined Diffraction and Gas Adsorption Experiment. Inorganic Chemistry, 2014, 53, 1513-1520.	4.0	43
282	Nonlinear Optical Switching in Regioregular Porphyrin Covalent Organic Frameworks. Angewandte Chemie, 2019, 131, 6970-6974.	2.0	43
283	Scalable production of nitrogen-doped carbons for multilayer lithium-sulfur battery cells. Carbon, 2020, 161, 190-197.	10.3	43
284	Preparation of BaTiO3 nanocrystals using a two-phase solvothermal method. Journal of Materials Chemistry, 2007, 17, 4605.	6.7	42
285	Atomic Sn–enabled high-utilization, large-capacity, and long-life Na anode. Science Advances, 2022, 8, eabm7489.	10.3	42
286	Hyperbranched Polymer/TiO2 Hybrid Nanoparticles Synthesized via an In Situ Sol-Gel Process. Macromolecular Chemistry and Physics, 2007, 208, 76-86.	2.2	41
287	Characteristics of flexibility in metal-organic framework solid solutions of composition [Zn2(BME-bdc)x(DB-bdc)2â^²xdabco]n: In situ powder X-ray diffraction, in situ NMR spectroscopy, and molecular dynamics simulations. Microporous and Mesoporous Materials, 2015, 216, 64-74.	4.4	41
288	In Situ Monitoring of Unique Switching Transitions in the Pressure-Amplifying Flexible Framework Material DUT-49 by High-Pressure <sup>129</sup> Xe NMR Spectroscopy. Journal of Physical Chemistry C, 2017, 121, 5195-5200.	3.1	41

#	Article	IF	CITATIONS
289	High-Pressure in Situ <sup>129</sup> Xe NMR Spectroscopy: Insights into Switching Mechanisms of Flexible Metal–Organic Frameworks Isoreticular to DUT-49. Chemistry of Materials, 2019, 31, 6193-6201.	6.7	41
290	Zn and Co redox active coordination polymers as efficient electrocatalysts. Dalton Transactions, 2019, 48, 3601-3609.	3.3	41
291	From Macro- to Nanoscale: Finite Size Effects on Metal–Organic Framework Switchability. Trends in Chemistry, 2021, 3, 291-304.	8.5	41
292	Preparation of luminescent ZnS:Cu nanoparticles for the functionalization of transparent acrylate polymers. Journal of Luminescence, 2010, 130, 692-697.	3.1	40
293	EPR Insights into Switchable and Rigid Derivatives of the Metal–Organic Framework DUT-8(Ni) by NO Adsorption. Journal of Physical Chemistry C, 2016, 120, 14246-14259.	3.1	40
294	Importance of Capacity Balancing on The Electrochemical Performance of Li[Ni <sub>0.8</sub> Co <sub>0.1</sub> Mn <sub>0.1</sub> ]O <sub>2</sub> (NCM811)/Silicon Full Cells. Journal of the Electrochemical Society, 2019, 166, A3265-A3271.	2.9	40
295	Towards highly active and stable nickel-based metal–organic frameworks as ethylene oligomerization catalysts. Dalton Transactions, 2019, 48, 3415-3421.	3.3	40
296	Sodium Sulfide Cathodes Superseding Hard Carbon Preâ€sodiation for the Production and Operation of Sodium–Sulfur Batteries at Room Temperature. Advanced Energy Materials, 2020, 10, 1903245.	19.5	40
297	Chemically Stable Carbazole-Based Imine Covalent Organic Frameworks with Acidochromic Response for Humidity Control Applications. Journal of the American Chemical Society, 2021, 143, 18368-18373.	13.7	40
298	Synthesis of mesoporous silicon imido nitride with high surface area and narrow pore size distribution. Chemical Communications, 2000, , 2481-2482.	4.1	39
299	Synthesis and Structure of K10Tl7:Â The First Binary Trielide Containing Naked Pentagonal Bipyramidal Tl7Clusters. Inorganic Chemistry, 2000, 39, 778-782.	4.0	39
300	Surface functionalization of ZrO2 nanocrystallites for the integration into acrylate nanocomposite films. Journal of Colloid and Interface Science, 2008, 323, 84-91.	9.4	39
301	New Element Organic Frameworks Based on Sn, Sb, and Bi, with Permanent Porosity and High Catalytic Activity. Materials, 2010, 3, 2447-2462.	2.9	39
302	In-Depth Investigation of the Carbon Microstructure of Silicon Carbide-Derived Carbons by Wide-Angle X-ray Scattering. Journal of Physical Chemistry C, 2014, 118, 15705-15715.	3.1	39
303	An In Situ Sourceâ€Templateâ€Interface Reaction Route to 3D Nitrogenâ€Doped Hierarchical Porous Carbon as Oxygen Reduction Electrocatalyst. Advanced Materials Interfaces, 2015, 2, 1500199.	3.7	39
304	Vapochromic Luminescence of a Zirconiumâ€Based Metal–Organic Framework for Sensing Applications. European Journal of Inorganic Chemistry, 2016, 2016, 4483-4489.	2.0	39
305	Surface and Electrochemical Studies on Silicon Diphosphide as Easy-to-Handle Anode Material for Lithium-Based Batteries—the Phosphorus Path. ACS Applied Materials & Interfaces, 2018, 10, 7096-7106.	8.0	39
306	Conformational isomerism controls collective flexibility in metal–organic framework DUT-8(Ni). Physical Chemistry Chemical Physics, 2019, 21, 674-680.	2.8	39

6.7

35

#	Article	IF	CITATIONS
307	A Universal Standard Archive File for Adsorption Data. Langmuir, 2021, 37, 4222-4226.	3.5	39
308	The Chemistry of Metal-Organic Frameworks: Synthesis, Characterization, and Applications. , 2016, , .		39
309	Porous CeO <sub><i>X</i></sub> /SiC Nanocomposites Prepared from Reverse Polycarbosilane-Based Microemulsions. Chemistry of Materials, 2008, 20, 77-83.	6.7	38
310	Chiral recognition in metal–organic frameworks studied by solid-state NMR spectroscopy using chiral solvating agents. Chemical Communications, 2012, 48, 10484.	4.1	38
311	Trimodal hierarchical carbide-derived carbon monoliths from steam- and CO <sub>2</sub> -activated wood templates for high rate lithium sulfur batteries. Journal of Materials Chemistry A, 2015, 3, 24103-24111.	10.3	38
312	Hierarchical columnar silicon anode structures for high energy density lithium sulfur batteries. Journal of Power Sources, 2017, 351, 183-191.	7.8	38
313	MIL-53(Al)/Carbon Films for CO <sub>2</sub> -Sensing at High Pressure. ACS Sustainable Chemistry and Engineering, 2019, 7, 4012-4018.	6.7	38
314	New Polymorphs of Magnesium-Based Metal–Organic Frameworks Mg3(ndc)3 (ndc =) Tj ETQq0 0 0 rgBT /Ove	rlock 10 Ti 2.0	f 5 <u>0</u> 462 Td (2
315	Wet-chemical catalyst deposition for scalable synthesis of vertical aligned carbon nanotubes on metal substrates. Chemical Physics Letters, 2011, 511, 288-293.	2.6	37
316	In Situ <sup>13</sup> C NMR Spectroscopy Study of CO <sub>2</sub> /CH <sub>4</sub> Mixture Adsorption by Metal–Organic Frameworks: Does Flexibility Influence Selectivity?. Langmuir, 2019, 35, 3162-3170.	3.5	37
317	Piezoelectric Inkjet Printing of Nanoporous Carbons for Micro-supercapacitor Devices. ACS Applied Energy Materials, 2021, 4, 1560-1567.	5.1	37
318	Topological Diversity, Adsorption and Fluorescence Properties of MOFs Based on a Tetracarboxylate Ligand. European Journal of Inorganic Chemistry, 2010, 2010, 3835-3841.	2.0	36
319	Hydrogen production from catalytic decomposition of methane over ordered mesoporous carbons (CMK-3) and carbide-derived carbon (DUT-19). Carbon, 2014, 67, 377-389.	10.3	36
320	Gold Nanoparticle-Decorated Diatom Biosilica: A Favorable Catalyst for the Oxidation of <scp>d</scp> -Glucose. ACS Omega, 2016, 1, 1253-1261.	3.5	36
321	Nitrogen doped carbide derived carbon aerogels by chlorine etching of a SiCN aerogel. Journal of Materials Chemistry A, 2016, 4, 4525-4533.	10.3	36
322	Influence of precursor porosity on sodium and sulfur promoted iron/carbon Fischer–Tropsch catalysts derived from metal–organic frameworks. Chemical Communications, 2017, 53, 10204-10207.	4.1	36
323	Synthesis of MNbO3Nanoparticles (M = Li, Na, K). Chemistry of Materials, 2006, 18, 4227-4230.	6.7	35
394	Design of Hierarchically Porous Carbons with Interlinked Hydrophilic and Hydrophobic Surface and	67	25

<sup>324</sup> Design of Hierarchically Porous Carbons with Interlinked Hydrophilic and Hydrophobic Surface and Their Capacitive Behavior. Chemistry of Materials, 2016, 28, 8715-8725.

#	Article	IF	CITATIONS
325	Three-dimensional ordered mesoporous cobalt nitride for fast-kinetics and stable-cycling lithium storage. Journal of Materials Chemistry A, 2019, 7, 17561-17569.	10.3	35
326	Classification of Black Plastics Waste Using Fluorescence Imaging and Machine Learning. Recycling, 2019, 4, 40.	5.0	35
327	Nanocasting Route to Ordered Mesoporous Carbon with FePt Nanoparticles and Its Phenol Adsorption Property. Journal of Physical Chemistry C, 2009, 113, 5998-6002.	3.1	34
328	Structural Study of D2 within the Trimodal Pore System of a Metal Organic Framework. Journal of Physical Chemistry C, 2011, 115, 8851-8857.	3.1	34
329	Mesoporous CeO <sub>2</sub> nanoparticles synthesized by an inverse miniemulsion technique and their catalytic properties in methane oxidation. Nanotechnology, 2011, 22, 135606.	2.6	34
330	Polymeric Frameworks as Organic Semiconductors with Controlled Electronic Properties. Journal of Physical Chemistry Letters, 2013, 4, 2977-2981.	4.6	34
331	Reversible Water-Induced Structural and Magnetic Transformations and Selective Water Adsorption Properties of Poly(manganese 1,1′-ferrocenediyl-bis(H-phosphinate)). Crystal Growth and Design, 2016, 16, 5084-5090.	3.0	34
332	Tuning the flexibility in MOFs by SBU functionalization. Dalton Transactions, 2016, 45, 4407-4415.	3.3	34
333	Mesoporous Thin-Wall Molybdenum Nitride for Fast and Stable Na/Li Storage. ACS Applied Materials & Interfaces, 2019, 11, 41188-41195.	8.0	34
334	Liquid-phase adsorption on metal-organic frameworks. Adsorption, 2011, 17, 219-226.	3.0	33
335	Porous phosphorus-based element organic frameworks: A new platform for transition metal catalysts immobilization. Microporous and Mesoporous Materials, 2013, 172, 167-173.	4.4	33
336	Electrolyte mobility in supercapacitor electrodes – Solid state NMR studies on hierarchical and narrow pore sized carbons. Energy Storage Materials, 2018, 12, 183-190.	18.0	33
337	Insights into the role of zirconium in proline functionalized metal-organic frameworks attaining high enantio- and diastereoselectivity. Journal of Catalysis, 2019, 377, 41-50.	6.2	33
338	Cooperative light-induced breathing of soft porous crystals via azobenzene buckling. Nature Communications, 2022, 13, 1951.	12.8	33
339	Out-of-furnace oxidation of SiCN polymer-derived ceramic aerogel pyrolized at intermediate temperature (600–800 °C). Journal of the European Ceramic Society, 2016, 36, 423-428.	5.7	32
340	Optical and thermal properties of transparent infrared blocking antimony doped tin oxide thin films. Thin Solid Films, 2017, 624, 152-159.	1.8	32
341	Poren per Baukasten. Nachrichten Aus Der Chemie, 2005, 53, 394-399.	0.0	31
342	Structural Characterization of Micro- and Mesoporous Carbon Materials Using In Situ High Pressure <sup>129</sup> Xe NMR Spectroscopy. Chemistry of Materials, 2014, 26, 3280-3288.	6.7	31

#	Article	IF	CITATIONS
343	A smart magnetic nanosystem with controllable drug release and hyperthermia for potential cancer therapy. RSC Advances, 2015, 5, 99875-99883.	3.6	31
344	Impact of Defects and Crystal Size on Negative Gas Adsorption in DUT-49 Analyzed by <i>In Situ</i> <sup>129</sup> Xe NMR Spectroscopy. Chemistry of Materials, 2020, 32, 4641-4650.	6.7	31
345	Ultra-hydrophilic porous carbons and their supercapacitor performance using pure water as electrolyte. Carbon, 2021, 178, 540-551.	10.3	31
346	Self-Assembly of Colloidal Zeolite Precursors into Extended Hierarchically Ordered Solids. Chemistry of Materials, 2004, 16, 3139-3146.	6.7	30
347	Preparation of photochromic transparent BiOX (X = Cl, I)/PLA nanocomposite materials via microemulsion polymerization. Journal of Materials Chemistry, 2007, 17, 4964.	6.7	30
348	Infrasorb: Optical detection of the heat of adsorption for high throughput adsorption screening of porous solids. Microporous and Mesoporous Materials, 2012, 149, 86-94.	4.4	30
349	Diffusion Study by IR Micro-Imaging of Molecular Uptake and Release on Mesoporous Zeolites of Structure Type CHA and LTA. Materials, 2013, 6, 2662-2688.	2.9	30
350	Textural Characterization of Micro- and Mesoporous Carbons Using Combined Gas Adsorption and <i>n</i> -Nonane Preadsorption. Langmuir, 2013, 29, 8133-8139.	3.5	30
351	Coprecipitation of Oxalates: An Easy and Reproducible Wetâ€Chemistry Synthesis Route for Transitionâ€Metal Ferrites. European Journal of Inorganic Chemistry, 2014, 2014, 875-887.	2.0	30
352	Engineering micromechanics of soft porous crystals for negative gas adsorption. Chemical Science, 2020, 11, 9468-9479.	7.4	30
353	Generalized Domino-Driven Synthesis of Hollow Hybrid Carbon Spheres with Ultrafine Metal Nitrides/Oxides. Matter, 2020, 3, 246-260.	10.0	30
354	The role of diffusion processes in the self-discharge of electrochemical capacitors. Energy Storage Materials, 2021, 37, 501-508.	18.0	30
355	Synthesis, Structure, and Properties of Bi3.25Pr0.75Ti2.97V0.03O12Ferroelectric Ceramics. Journal of Physical Chemistry C, 2007, 111, 11095-11103.	3.1	29
356	Insights into the redistribution of sulfur species during cycling in lithium-sulfur batteries using physisorption methods. Nano Energy, 2017, 34, 437-441.	16.0	29
357	Highly dispersed metal and oxide nanoparticles on ultra-polar carbon as efficient cathode materials for Li–O <sub>2</sub> batteries. Journal of Materials Chemistry A, 2017, 5, 6284-6291.	10.3	29
358	Amine assisted top-down delamination of the two-dimensional metal–organic framework Cu <sub>2</sub> (bdc) <sub>2</sub> . Dalton Transactions, 2017, 46, 16480-16484.	3.3	29
359	Anion Exchange and Catalytic Functionalization of the Zirconium-Based Metal–Organic Framework DUT-67. Crystal Growth and Design, 2018, 18, 5492-5500.	3.0	29
360	Exploring the thermodynamic criteria for responsive adsorption processes. Chemical Science, 2019, 10, 5011-5017.	7.4	29

#	Article	IF	CITATIONS
361	Manipulation of carbon framework from the microporous to nonporous via a mechanical-assisted treatment for structure-oriented energy storage. Carbon, 2020, 159, 140-148.	10.3	29
362	Tailoring the Adsorption-Induced Flexibility of a Pillared Layer Metal–Organic Framework DUT-8(Ni) by Cobalt Substitution. Chemistry of Materials, 2020, 32, 5670-5681.	6.7	29
363	1 H– 13 C– 29 Si triple resonance and REDOR solid-state NMR—A tool to study interactions between biosilica and organic molecules in diatom cell walls. Solid State Nuclear Magnetic Resonance, 2015, 66-67, 33-39.	2.3	28
364	High-power lithium ion batteries based on preorganized necklace type Li4Ti5O12/VACNT nano-composites. Journal of Power Sources, 2016, 325, 1-6.	7.8	28
365	Zinc-salt templating of hierarchical porous carbons for low electrolyte high energy lithium-sulfur batteries (LE-LiS). Carbon, 2016, 107, 705-710.	10.3	28
366	The impact of crystal size and temperature on the adsorption-induced flexibility of the Zr-based metal–organic framework DUT-98. Beilstein Journal of Nanotechnology, 2019, 10, 1737-1744.	2.8	28
367	Designing room temperature sodium sulfur batteries with long cycle-life at pouch cell level. Energy Storage Materials, 2019, 21, 41-49.	18.0	28
368	Combining <i>In Situ</i> Techniques (XRD, IR, and <sup>13</sup> C NMR) and Gas Adsorption Measurements Reveals CO <sub>2</sub> -Induced Structural Transitions and High CO <sub>2</sub> /CH <sub>4</sub> Selectivity for a Flexible Metal–Organic Framework JUK-8. ACS Applied Materials & Interfaces, 2021, 13, 28503-28513.	8.0	28
369	Isotope-selective pore opening in a flexible metal-organic framework. Science Advances, 2022, 8, eabn7035.	10.3	28
370	Titanium terephthalate (TT-1) hybrid materials with high specific surface area. Journal of Materials Chemistry, 2006, 16, 2354-2357.	6.7	27
371	Mesoporous Ferromagnetic MPt@Silica/Carbon (M = Fe, Co, Ni) Composites As Advanced Bifunctional Catalysts. Chemistry of Materials, 2010, 22, 1624-1632.	6.7	27
372	Kroll-carbons based on silica and alumina templates as high-rate electrode materials in electrochemical double-layer capacitors. Journal of Materials Chemistry A, 2014, 2, 5131.	10.3	27
373	Evolution of porosity in carbide-derived carbon aerogels. Journal of Materials Chemistry A, 2014, 2, 18472-18479.	10.3	27
374	Advanced Structural Analysis of Nanoporous Materials by Thermal Response Measurements. Langmuir, 2015, 31, 4040-4047.	3.5	27
375	Selective absorption of Carbon Nanotube thin films for solar energy applications. Solar Energy Materials and Solar Cells, 2015, 143, 553-556.	6.2	27
376	Carboxylate-Hydrazone Mixed-Linker Metal-Organic Frameworks: Synthesis, Structure, and Selective Gas Adsorption. European Journal of Inorganic Chemistry, 2016, 2016, 4450-4456.	2.0	27
377	Assessing negative thermal expansion in mesoporous metal–organic frameworks by molecular simulation. Journal of Materials Chemistry A, 2019, 7, 24019-24026.	10.3	27
378	Structural diversity of cobalt(II) coordination compounds involving bent imidazole ligand: A route from 0D dimer to 3D coordination polymer. Polyhedron, 2012, 44, 179-186.	2.2	26

#	Article	IF	CITATIONS
379	An Isoreticular Family of Microporous Metal–Organic Frameworks Based on Zinc and 2â€Substituted Imidazolateâ€4â€amideâ€5â€imidate: Syntheses, Structures and Properties. Chemistry - A European Journal, 20 18, 11630-11640.	)12,3.3	26
380	A series of amide functionalized isoreticular metal organic frameworks. Microporous and Mesoporous Materials, 2014, 194, 115-125.	4.4	26
381	Guest Adsorption in the Nanoporous Metal–Organic Framework Cu3(1,3,5-Benzenetricarboxylate)2: Combined In Situ X-ray Diffraction and Vapor Sorption. Chemistry of Materials, 2014, 26, 4712-4723.	6.7	26
382	Hierarchical Tiâ€Beta Obtained by Simultaneous Desilication and Titanation as an Efficient Catalyst for Cyclooctene Epoxidation. ChemCatChem, 2017, 9, 3860-3869.	3.7	26
383	Silicon monophosphide as a possible lithium battery anode material. Journal of Materials Chemistry A, 2018, 6, 19974-19978.	10.3	26
384	Synthesis, Structure, and Bonding of A5Cd2Tl11, A = Cs, Rb. Naked Pentagonal Antiprismatic Columns Centered by Cadmium. Inorganic Chemistry, 2000, 39, 3086-3091.	4.0	25
385	Formation of SiC nanoparticles in an atmospheric microwave plasma. Beilstein Journal of Nanotechnology, 2011, 2, 665-673.	2.8	25
386	A family of 2D and 3D coordination polymers involving a trigonal tritopic linker. Dalton Transactions, 2012, 41, 4172.	3.3	25
387	Semi-transparent silver electrodes for flexible electronic devices prepared by nanoimprint lithography. Journal of Materials Chemistry C, 2013, 1, 638-645.	5.5	25
388	Electroless copper deposition on (3-mercaptopropyl)triethoxysilane-coated silica and alumina nanoparticles. Electrochimica Acta, 2013, 114, 521-526.	5.2	25
389	Isophthalate–Hydrazone 2D Zinc–Organic Framework: Crystal Structure, Selective Adsorption, and Tuning of Mechanochemical Synthetic Conditions. Inorganic Chemistry, 2016, 55, 9663-9670.	4.0	25
390	Mechanische Stabilitäversus ultrahohe Porositäin kristallinen Netzwerkmaterialien: ein Balanceakt!. Angewandte Chemie, 2018, 130, 13976-13979.	2.0	25
391	Screening of Porous Materials by Thermal Response Measurements. Chemie-Ingenieur-Technik, 2013, 85, 747-752.	0.8	24
392	Topological control of 3,4-connected frameworks based on the Cu <sub>2</sub> -paddle-wheel node: <b>tbo</b> or <b>pto</b> , and why?. CrystEngComm, 2016, 18, 8164-8171.	2.6	24
393	Gas Storage Applications. Crystal Growth and Design, 2017, 17, 3221-3228.	3.0	24
394	Computational screening, synthesis and testing of metal–organic frameworks with a bithiazole linker for carbon dioxide capture and its green conversion into cyclic carbonates. Molecular Systems Design and Engineering, 2019, 4, 1000-1013.	3.4	24
395	A new type of alumoxane obtained by controlled hydrolysis of N,N-dialkylcarbamato complexes of aluminium; crystal and molecular structure of [Al4(µ3-O)2(O2CNPri2)8]. Chemical Communications, 1997, , 1941.	4.1	23
396	Porosity control in pre-ceramic molecular precursor-derived GaN based materials. Journal of Materials Chemistry, 2004, 14, 1017.	6.7	23

#	Article	IF	CITATIONS
397	Integration of Zinc Oxide Nanoparticles into Transparent Poly(butanediolmonoacrylate) via Photopolymerisation. Journal of Nanoscience and Nanotechnology, 2006, 6, 409-413.	0.9	23
398	Synthesis and characterization of high surface area molybdenum nitride. Journal of Materials Science, 2006, 41, 2465-2470.	3.7	23
399	Ordered Mesoporous Boron Carbide Based Materials via Precursor Nanocasting. Chemistry of Materials, 2010, 22, 4660-4668.	6.7	23
400	Semimetallic Paramagnetic Nanoâ€Bi <sub>2</sub> Ir and Superconducting Ferromagnetic Nanoâ€Bi <sub>3</sub> Ni by Microwaveâ€Assisted Synthesis and Room Temperature Pseudomorphosis. Zeitschrift Fur Anorganische Und Allgemeine Chemie, 2012, 638, 2035-2043.	1.2	23
401	Sulfur Cathodes with Carbon Current Collector for Li-S cells. Journal of the Electrochemical Society, 2013, 160, A996-A1002.	2.9	23
402	Thermogravimetric Analysis of Activated Carbons, Ordered Mesoporous Carbide-Derived Carbons, and Their Deactivation Kinetics of Catalytic Methane Decomposition. Industrial & Engineering Chemistry Research, 2014, 53, 1741-1753.	3.7	23
403	Emulsion soft templating of carbide-derived carbon nanospheres with controllable porosity for capacitive electrochemical energy storage. Journal of Materials Chemistry A, 2015, 3, 17983-17990.	10.3	23
404	The origin of the measured chemical shift of <sup>129</sup> Xe in UiO-66 and UiO-67 revealed by DFT investigations. Physical Chemistry Chemical Physics, 2017, 19, 10020-10027.	2.8	23
405	Switchable Supercapacitors with Transistorâ€Like Gating Characteristics (Gâ€Cap). Advanced Functional Materials, 2020, 30, 1910439.	14.9	23
406	New 1D chiral Zr-MOFs based on in situ imine linker formation as catalysts for asymmetric C C coupling reactions. Journal of Catalysis, 2020, 386, 106-116.	6.2	23
407	Tailoring adsorption induced switchability of a pillared layer MOF by crystal size engineering. CrystEngComm, 2021, 23, 538-549.	2.6	23
408	Liquid lithium metal processing into ultrathin metal anodes for solid state batteries. Chemical Engineering Journal Advances, 2022, 9, 100218.	5.2	23
409	Functionalised porous nanocomposites: a multidisciplinary approach to investigate designed structures for supercapacitor applications. Journal of Materials Chemistry A, 2013, 1, 4904.	10.3	22
410	Nanoporous silicon carbide as nickel support for the carbon dioxide reforming of methane. Catalysis Science and Technology, 2015, 5, 4174-4183.	4.1	22
411	Carbon nano-composites for lithium–sulfur batteries. Current Opinion in Green and Sustainable Chemistry, 2017, 4, 64-71.	5.9	22
412	Enabling electrolyte compositions for columnar silicon anodes in high energy secondary batteries. Journal of Power Sources, 2017, 362, 349-357.	7.8	22
413	Are Diatoms "Green―Aluminosilicate Synthesis Microreactors for Future Catalyst Production?. Molecules, 2017, 22, 2232.	3.8	22
414	Selective Alcohol Electrooxidation by ZIF-8 Functionalized Pt/Carbon Catalyst. ACS Applied Materials & Interfaces, 2019, 11, 20915-20922.	8.0	22

#	Article	IF	CITATIONS
415	Facile regulation of carbon framework from the microporous to low-porous via molecular crosslinker design and enhanced Na storage. Carbon, 2020, 167, 896-905.	10.3	22
416	Impact of Carbon Porosity on Sulfur Conversion in Liâ´'S Battery Cathodes in a Sparingly Polysulfide Solvating Electrolyte. Batteries and Supercaps, 2021, 4, 823-833.	4.7	22
417	Impact of Crystal Size and Morphology on Switchability Characteristics in Pillared-Layer Metal-Organic Framework DUT-8(Ni). Frontiers in Chemistry, 2021, 9, 674566.	3.6	22
418	Template assisted design of microporous gallium nitride materials. Chemical Communications, 2003, , 730.	4.1	21
419	Tailoring structural and electrochemical properties of vertical aligned carbon nanotubes on metal foil using scalable wet-chemical catalyst deposition. Journal of Power Sources, 2012, 208, 426-433.	7.8	21
420	Titanium Carbide and Carbideâ€Đerived Carbon Composite Nanofibers by Electrospinning of Tiâ€Resin Precursor. Chemie-Ingenieur-Technik, 2013, 85, 1742-1748.	0.8	21
421	The modulator driven polymorphism of Zr(IV) based metal–organic frameworks. Philosophical Transactions Series A, Mathematical, Physical, and Engineering Sciences, 2017, 375, 20160027.	3.4	21
422	Sulfur: an intermediate template for advanced silicon anode architectures. Journal of Materials Chemistry A, 2018, 6, 14787-14796.	10.3	21
423	Quantitative <i>in situ</i> <sup>13</sup> C NMR studies of the electro-catalytic oxidation of ethanol. Chemical Communications, 2019, 55, 6042-6045.	4.1	21
424	Ionic liquid - Electrode materials interactions studied by NMR spectroscopy, cyclic voltammetry, and impedance spectroscopy. Energy Storage Materials, 2019, 19, 432-438.	18.0	21
425	Efficiency of Light Outcoupling Structures in Organic Lightâ€Emitting Diodes: 2D TiO <sub>2</sub> Array as a Model System. Advanced Functional Materials, 2019, 29, 1901748.	14.9	21
426	Charting the Complete Thermodynamic Landscape of Gas Adsorption for a Responsive Metal–Organic Framework. Journal of the American Chemical Society, 2021, 143, 4143-4147.	13.7	21
427	Nanoimprint patterning of thin cadmium stannate films using a polymeric precursor route. Journal of Materials Chemistry, 2011, 21, 10697.	6.7	20
428	Polymer-derived nanoporous silicon carbide with monodisperse spherical pores. Journal of Materials Chemistry, 2012, 22, 24841.	6.7	20
429	Preparation of cubic ordered mesoporous silicon carbide monoliths by pressure assisted preceramic polymer nanocasting. Microporous and Mesoporous Materials, 2013, 168, 142-147.	4.4	20
430	ZnPd/ZnO Aerogels as Potential Catalytic Materials. Advanced Functional Materials, 2016, 26, 1014-1020.	14.9	20
431	Towards a continuous adsorption process for the enrichment of ACE-inhibiting peptides from food protein hydrolysates. Carbon, 2016, 107, 116-123.	10.3	20
432	Nanoporous polymers as highly sensitive functional material in chemiresistive gas sensors. Sensors and Actuators B: Chemical, 2016, 223, 166-171.	7.8	20

#	Article	IF	CITATIONS
433	Bioinspired carbide-derived carbons with hierarchical pore structure for the adsorptive removal of mercury from aqueous solution. Chemical Communications, 2017, 53, 4845-4848.	4.1	20
434	Effect of Linker Substituent on Layers Arrangement, Stability, and Sorption of Zn-Isophthalate/Acylhydrazone Frameworks. Crystal Growth and Design, 2018, 18, 488-497.	3.0	20
435	New insights into solvent-induced structural changes of <sup>13</sup> C labelled metal–organic frameworks by solid state NMR. Chemical Communications, 2019, 55, 9140-9143.	4.1	20
436	Synthesis of Ordered Mesoporous Carbon Materials by Dry Etching. Chemistry - A European Journal, 2015, 21, 14753-14757.	3.3	19
437	Optical Sensors Using Solvatochromic Metal–Organic Frameworks. Inorganic Chemistry, 2017, 56, 14164-14169.	4.0	19
438	Salt templated synthesis of hierarchical covalent triazine frameworks. Microporous and Mesoporous Materials, 2017, 239, 190-194.	4.4	19
439	Ultrastable Surfaceâ€Dominated Pseudocapacitive Potassium Storage Enabled by Edgeâ€Enriched Nâ€Doped Porous Carbon Nanosheets. Angewandte Chemie, 2020, 132, 19628-19635.	2.0	19
440	The role of temperature and adsorbate on negative gas adsorption transitions of the mesoporous metal–organic framework DUT-49. Faraday Discussions, 2021, 225, 168-183.	3.2	19
441	Porphyrinâ€basierte Metallâ€organische Gerüste für biomedizinische Anwendungen. Angewandte Chemie, 2021, 133, 5064-5091.	2.0	19
442	Nanostructured Siâ^'C Composites As Highâ€Capacity Anode Material For Allâ€Solidâ€State Lithiumâ€lon Batteries**. Batteries and Supercaps, 2021, 4, 1323-1334.	4.7	19
443	Refractive index tuning of highly transparent bismuth containing polymer composites. Polymer, 2011, 52, 3263-3268.	3.8	18
444	Total Synthesis and Biological Activity of the Proposed Structure of Phaeosphaeride A. Journal of Organic Chemistry, 2012, 77, 9659-9667.	3.2	18
445	Modular Construction of a Porous Organometallic Network Based on Rhodium Olefin Complexation. Journal of the American Chemical Society, 2012, 134, 17335-17337.	13.7	18
446	Preparation of hierarchical porous biomorphic carbide-derived carbon by polycarbosilane impregnation of wood. Microporous and Mesoporous Materials, 2015, 210, 26-31.	4.4	18
447	Guest–Host Complexes of TCNQ and TCNE with Cu <sub>3</sub> (1,3,5-benzenetricarboxylate) <sub>2</sub> . Journal of Physical Chemistry C, 2017, 121, 26330-26339.	3.1	18
448	In Situ Imine-Based Linker Formation for the Synthesis of Zirconium MOFs: A Route to CO <sub>2</sub> Capture Materials and Ethylene Oligomerization Catalysts. Inorganic Chemistry, 2020, 59, 350-359.	4.0	18
449	The Role of Carbon Electrodes Pore Size Distribution on the Formation of the Cathode–Electrolyte Interphase in Lithium–Sulfur Batteries. Batteries and Supercaps, 2021, 4, 612-622.	4.7	18
450	Hierarchical porous zeolite ZSM-58 derived by desilication and desilication re-assembly. Microporous and Mesoporous Materials, 2014, 187, 114-124.	4.4	17

#	Article	IF	CITATIONS
451	Continuous electrooxdiation of sulfuric acid on boron-doped diamond electrodes. Electrochimica Acta, 2014, 147, 589-595.	5.2	17
452	Interactions Between Electrolytes and Carbon-Based Materials—NMR Studies on Electrical Double-Layer Capacitors, Lithium-Ion Batteries, and Fuel Cells. Annual Reports on NMR Spectroscopy, 2016, , 237-318.	1.5	17
453	CFA-4 – a fluorinated metal–organic framework with exchangeable interchannel cations. Dalton Transactions, 2017, 46, 6745-6755.	3.3	17
454	Synthesis of the homochiral metal–organic framework DUT-129 based on a chiral dicarboxylate linker with 6 stereocenters. CrystEngComm, 2017, 19, 2494-2499.	2.6	17
455	Integration of an Nâ€Heterocyclic Carbene Precursor into a Covalent Triazine Framework for Organocatalysis. Chemistry - A European Journal, 2018, 24, 18629-18633.	3.3	17
456	A Facile Strategy to Improve the Electrochemical Performance of Porous Organic Polymerâ€Based Lithium–Sulfur Batteries. Energy Technology, 2019, 7, 1900583.	3.8	17
457	Introducing a Longer versus Shorter Acylhydrazone Linker to a Metal–Organic Framework: Parallel Mechanochemical Approach, Nonisoreticular Structures, and Diverse Properties. Crystal Growth and Design, 2019, 19, 7160-7169.	3.0	17
458	Synthesis and Characterization of Cu–Ni Mixed Metal Paddlewheels Occurring in the Metal–Organic Framework DUT-8(Ni <sub>0.98</sub> Cu <sub>0.02</sub> ) for Monitoring Open-Closed-Pore Phase Transitions by X-Band Continuous Wave Electron Paramagnetic Resonance Spectroscopy. Inorganic Chemistry, 2019, 58, 4561-4573.	4.0	17
459	Measuring water adsorption processes of metal-organic frameworks for heat pump applications via optical calorimetry. Microporous and Mesoporous Materials, 2019, 278, 206-211.	4.4	17
460	Recent progress on the design of hollow carbon spheres to host sulfur in room-temperature sodium–sulfur batteries. New Carbon Materials, 2020, 35, 630-645.	6.1	17
461	Polyatomic Clusters of the Triel Elements. Palladium-Centered Clusters of Thallium in A8Tl11Pd, A = Cs, Rb, K. Inorganic Chemistry, 2002, 41, 3457-3462.	4.0	16
462	CeO <sub>2</sub> /Pt Catalyst Nanoparticle Containing Carbide-Derived Carbon Composites by a New In situ Functionalization Strategy. Chemistry of Materials, 2011, 23, 57-66.	6.7	16
463	Water-Stable Metal–Organic Framework with Three Hydrogen-Bond Acceptors: Versatile Theoretical and Experimental Insights into Adsorption Ability and Thermo-Hydrolytic Stability. Inorganic Chemistry, 2018, 57, 3287-3296.	4.0	16
464	Symmetric Lithium Sulfide – Sulfur Cells: A Method to Study Degradation Mechanisms of Cathode, Separator and Electrolyte Concepts for Lithium-Sulfur Batteries. Journal of the Electrochemical Society, 2018, 165, A1084-A1091.	2.9	16
465	Selective Adsorption of Propene over Propane on Hierarchical Zeolite ZSM-58. Industrial & Engineering Chemistry Research, 2018, 57, 6609-6617.	3.7	16
466	Selective pore opening and gating of the pillared layer metal-organic framework DUT-8(Ni) upon liquid phase multi-component adsorption. Microporous and Mesoporous Materials, 2018, 271, 169-174.	4.4	16
467	Fabrication of micro- and submicrometer silver patterns by microcontact printing of mercaptosilanes and direct electroless metallization. Microelectronic Engineering, 2013, 104, 100-104.	2.4	15
468	The Formation and Morphology of Nanoparticle Supracrystals. Advanced Functional Materials, 2016, 26, 4890-4895.	14.9	15

#	Article	IF	CITATIONS
469	Elucidating the Formation and Transformation Mechanisms of the Switchable Metal–Organic Framework <b>ELM-11</b> by Powder and Single-Crystal EPR Study. Inorganic Chemistry, 2018, 57, 11920-11929.	4.0	15
470	Metal–Organic Frameworks and Their Applications. Chemistry - an Asian Journal, 2019, 14, 3450-3451.	3.3	15
471	Interlinker Hydrogen Bonds Govern CO <sub>2</sub> Adsorption in a Series of Flexible 2D Diacylhydrazone/Isophthalate-Based MOFs: Influence of Metal Center, Linker Substituent, and Activation Temperature. Inorganic Chemistry, 2020, 59, 10717-10726.	4.0	15
472	Guest size limitation in metal–organic framework crystal–glass composites. Journal of Materials Chemistry A, 2021, 9, 8386-8393.	10.3	15
473	Monitoring Dynamics, Structure, and Magnetism of Switchable Metal–Organic Frameworks via <sup>1</sup> Hâ€Detected MASâ€NMR. Angewandte Chemie - International Edition, 2021, 60, 21778-21783.	13.8	15
474	The force of MOFs: the potential of switchable metal–organic frameworks as solvent stimulated actuators. Chemical Communications, 2020, 56, 7411-7414.	4.1	15
475	Structure and Mechanical Properties of Transparent ZnO/PBDMA Nanocomposites. Journal of Nanoscience and Nanotechnology, 2009, 9, 2739-2745.	0.9	14
476	Metallorganische Gerüstverbindungen (MOFs). Chemie-Ingenieur-Technik, 2010, 82, 1019-1023.	0.8	14
477	Wet chemical preparation of YVO4:Eu thin films as red-emitting phosphor layers for fully transparent flat dielectric discharge lamp. Thin Solid Films, 2012, 520, 4297-4301.	1.8	14
478	Inverse silicon carbide replica of porous glasses. Microporous and Mesoporous Materials, 2014, 184, 1-6.	4.4	14
479	Hierarchical zeolite ZSM-58 as shape selective catalyst for methanol-to-olefins reaction. Microporous and Mesoporous Materials, 2018, 261, 51-57.	4.4	14
480	On the origin of mesopore collapse in functionalized porous carbons. Carbon, 2019, 149, 743-749.	10.3	14
481	Role of particle size and surface functionalisation on the flexibility behaviour of switchable metal–organic framework DUT-8(Ni). Journal of Materials Chemistry A, 2020, 8, 22703-22711.	10.3	14
482	Reversible switching between positive and negative thermal expansion in a metal–organic framework DUT-49. Journal of Materials Chemistry A, 2020, 8, 20420-20428.	10.3	14
483	Single particle Raman spectroscopy analysis of the metal–organic framework DUT-8(Ni) switching transition under hydrostatic pressure. Chemical Communications, 2020, 56, 8269-8272.	4.1	14
484	Inâ€Situ Generation of Electrolyte inside Pyridineâ€Based Covalent Triazine Frameworks for Direct Supercapacitor Integration. ChemSusChem, 2020, 13, 3192-3198.	6.8	14
485	Structural Transitions of the Metal–Organic Framework DUT-49(Cu) upon Physi- and Chemisorption Studied by <i>in Situ</i> Electron Paramagnetic Resonance Spectroscopy. Journal of Physical Chemistry Letters, 2020, 11, 5856-5862.	4.6	14
486	Mechanistic Insights into the Role of Covalent Triazine Frameworks as Cathodes in Lithiumâ€ <b>s</b> ulfur Batteries. Batteries and Supercaps, 2020, 3, 1069-1079.	4.7	14

#	Article	IF	CITATIONS
487	Sulfur Transfer Melt Infiltration for Highâ€Power Carbon Nanotube Sheets in Lithium‣ulfur Pouch Cells. Batteries and Supercaps, 2021, 4, 989-1002.	4.7	14
488	Massive Pressure Amplification by Stimulated Contraction of Mesoporous Frameworks**. Angewandte Chemie - International Edition, 2021, 60, 11735-11739.	13.8	14
489	Study of Ammonolysis Reactions within SituX-Ray Diffraction: Detection and Crystal Structure of Li0.84W1.16N2. Journal of Solid State Chemistry, 1998, 138, 154-159.	2.9	13
490	High surface area V–Mo–N materials synthesized from amine intercalated foams. Journal of Solid State Chemistry, 2008, 181, 935-942.	2.9	13
491	Novel Composite Spherical Granulates with Catalytic Outer Layer and Improved Conversion Efficiency and Selectivity. Chemical Engineering and Technology, 2012, 35, 769-775.	1.5	13
492	Nanoporous and Highly Active Silicon Carbide Supported CeO <sub>2</sub> â€Catalysts for the Methane Oxidation Reaction. Small, 2014, 10, 316-322.	10.0	13
493	Direct synthesis of carbide-derived carbon monoliths with hierarchical pore design by hard-templating. Journal of Materials Chemistry A, 2014, 2, 12703-12707.	10.3	13
494	Investigations of mussel-inspired polydopamine deposition on WC and Al 2 O 3 particles: The influence of particle size and material. Materials Chemistry and Physics, 2014, 148, 624-630.	4.0	13
495	A hard-templating route towards ordered mesoporous tungsten carbide and carbide-derived carbons. Microporous and Mesoporous Materials, 2014, 186, 163-167.	4.4	13
496	Extraction of ACE-inhibiting dipeptides from protein hydrolysates using porous carbon materials. Carbon, 2014, 77, 191-198.	10.3	13
497	Enhancing ACE-inhibition of food protein hydrolysates by selective adsorption using porous carbon materials. Carbon, 2015, 87, 309-316.	10.3	13
498	Metal–Organic Frameworks for Thin-Layer Chromatographic Applications. ACS Applied Materials & Interfaces, 2017, 9, 2006-2009.	8.0	13
499	Solvothermal synthesis of a bismuth/zinc mixed oxide material for H2S removal at room temperature: Synthesis, performance, characterization and regeneration ability. Materials Chemistry and Physics, 2017, 199, 329-339.	4.0	13
500	A photosensor based on lead-free perovskite-like methyl-ammonium bismuth iodide. Sensors and Actuators A: Physical, 2019, 291, 75-79.	4.1	13
501	Operando Radiography and Multimodal Analysis of Lithium–Sulfur Pouch Cells—Electrolyte Dependent Morphology Evolution at the Cathode. Advanced Energy Materials, 2022, 12, .	19.5	13
502	Polymerization of polycarbosilanes in high internal phase emulsions for the synthesis of macroporous silicon carbide catalysts (polyHIPE-SiC). Journal of Materials Chemistry, 2011, 21, 11936.	6.7	12
503	3D assembly of silica encapsulated semiconductor nanocrystals. Nanoscale, 2015, 7, 12713-12721.	5.6	12
504	Copolymerisation at work: the first example of a highly porous MOF comprising a triarylborane-based linker. CrystEngComm, 2015, 17, 307-312.	2.6	12

#	Article	IF	CITATIONS
505	Quality Control of Slot-Die Coated Aluminum Oxide Layers for Battery Applications Using Hyperspectral Imaging. Journal of Imaging, 2016, 2, 12.	3.0	12
506	Engineering pore ratio in hierarchical porous carbons towards high-rate and large-volumetric performances. Microporous and Mesoporous Materials, 2019, 282, 205-210.	4.4	12
507	Design of Functional Nanostructured Carbons for Advanced Heterogeneous Catalysts: A Review. Current Organic Chemistry, 2014, 18, 1262-1279.	1.6	12
508	Thin-film microextraction using the metal-organic framework DUT-52 for determining endocrine disrupting chemicals in cosmetics. Microchemical Journal, 2022, 181, 107685.	4.5	12
509	Synthesis, Characterization, and Catalytic Properties of High-Surface-Area Aluminum Silicon Nitride Based Materials. Chemistry of Materials, 2005, 17, 181-185.	6.7	11
510	Complete and partial oxidation of methane on ceria/platinum silicon carbide nanocomposites. Catalysis Science and Technology, 2012, 2, 139-146.	4.1	11
511	Coating of NIL printed polymeric templates with semiconductor nanoparticles in solution for the preparation of anisotropic inorganic structures. Materials Chemistry and Physics, 2016, 182, 450-458.	4.0	11
512	Tetrazole-Stabilized Gold Nanoparticles for Catalytic Applications. Zeitschrift Fur Physikalische Chemie, 2017, 231, 51-62.	2.8	11
513	Bulky substituent and solvent-induced alternative nodes for layered Cd–isophthalate/acylhydrazone frameworks. CrystEngComm, 2018, 20, 2841-2849.	2.6	11
514	Influence of silica architecture on the catalytic activity of immobilized glucose oxidase. Bioinspired, Biomimetic and Nanobiomaterials, 2019, 8, 72-80.	0.9	11
515	Powder sample-positioning system for neutron scattering allowing gas delivery in top-loading cryofurnaces. Journal of Applied Crystallography, 2016, 49, 705-711.	4.5	11
516	Zirconium-Based Metal–Organic Framework Mixed-Matrix Membranes as Analytical Devices for the Trace Analysis of Complex Cosmetic Samples in the Assessment of Their Personal Care Product Content. ACS Applied Materials & Interfaces, 2022, 14, 4510-4521.	8.0	11
517	Structural phase transitions in flexible DUT-8(Ni) under high hydrostatic pressure. Physical Chemistry Chemical Physics, 2022, 24, 3788-3798.	2.8	11
518	29-P-17-Zirconia nanoparticles in ordered mesoporous material SBA-15. Studies in Surface Science and Catalysis, 2001, , 315.	1.5	10
519	Reverse micelle-mediated synthesis of zirconia with enhanced surface area using alcothermal treatment. Journal of Materials Chemistry, 2006, 16, 391-394.	6.7	10
520	Themed issue: integrating functionality into metal–organic frameworks. Journal of Materials Chemistry, 2012, 22, 10093.	6.7	10
521	Atmospheric Plasma Deposition of SiO2 Films for Adhesion Promoting Layers on Titanium. Metals, 2014, 4, 639-646.	2.3	10
522	Tailoring Commercially Available Raw Materials for Lithium–Sulfur Batteries with Superior Performance and Enhanced Shelf Life. Energy Technology, 2015, 3, 1007-1013.	3.8	10

#	Article	IF	CITATIONS
523	Speeding Up Chemisorption Analysis by Direct IR-Heat-Release Measurements (Infrasorp Technology): A Screening Alternative to Breakthrough Measurements. Industrial & Engineering Chemistry Research, 2015, 54, 6677-6682.	3.7	10
524	Microemulsion flame pyrolysis for hopcalite nanoparticle synthesis: a new concept for catalyst preparation. Chemical Communications, 2015, 51, 5872-5875.	4.1	10
525	Stabilizing Effect of Polysulfides on Lithium Metal Anodes in Sparingly Solvating Solvents. Batteries and Supercaps, 2021, 4, 347-358.	4.7	10
526	Crystal growth in supercritical ammonia using high surface area silicon nitride feedstock. Journal of Crystal Growth, 2004, 261, 99-104.	1.5	9
527	Foam-derived multiferroic BiFeO <sub>3</sub> nanoparticles and integration into transparent polymer nanocomposites. Journal of Experimental Nanoscience, 2008, 3, 1-15.	2.4	9
528	Ordered Mesoporous Silica (OMS) Supported Vanadium Nitride and Carbide Catalysts. Topics in Catalysis, 2009, 52, 1549-1558.	2.8	9
529	In-Line Plasma-Chemical Etching of Crystalline Silicon Solar Wafers at Atmospheric Pressure. IEEE Transactions on Plasma Science, 2009, 37, 979-984.	1.3	9
530	Electrodeposition of copper on aligned multi-walled carbon nanotubes. Surface Engineering, 2012, 28, 435-441.	2.2	9
531	A New Silverâ€Based Precursor as Ink for Soft Printing Techniques. European Journal of Inorganic Chemistry, 2012, 2012, 878-883.	2.0	9
532	Reprint of "Structural diversity of cobalt(II) coordination compounds involving bent imidazole ligand: A route from 0D dimer to 3D coordination polymer― Polyhedron, 2013, 52, 1481-1488.	2.2	9
533	Fast patterning of poly(methyl methacrylate) by a novel soft molding approach and its application to the fabrication of silver structures. Materials Chemistry and Physics, 2013, 137, 884-891.	4.0	9
534	Zinc Coordination Polymers Containing Isomeric Forms of <i>p</i> â€(Thiazolyl)benzoic Acid: Blueâ€Emitting Materials with a Solvatochromic Response to Water. European Journal of Inorganic Chemistry, 2017, 2017, 4909-4918.	2.0	9
535	A Stimuliâ€Responsive Zirconium Metal–Organic Framework Based on Supermolecular Design. Angewandte Chemie, 2017, 129, 10816-10820.	2.0	9
536	Nanostructured Networks for Energy Storage: Vertically Aligned Carbon Nanotubes (VACNT) as Current Collectors for High-Power Li4Ti5O12(LTO)//LiMn2O4(LMO) Lithium-Ion Batteries. Batteries, 2017, 3, 37.	4.5	9
537	Rapid screening of zeolite acidity by thermal response measurements using InfraSORP technology. Microporous and Mesoporous Materials, 2018, 268, 46-49.	4.4	9
538	Hyperspectral Imaging Using Laser Excitation for Fast Raman and Fluorescence Hyperspectral Imaging for Sorting and Quality Control Applications. Journal of Imaging, 2018, 4, 110.	3.0	9
539	Tailoring Catalytic Properties of Copper Manganese Oxide Nanoparticles (Hopcalitesâ€2G) via Flame Spray Pyrolysis. ChemCatChem, 2018, 10, 3914-3922.	3.7	9
540	Function from configurational degeneracy in disordered framework materials. Faraday Discussions, 2021, 225, 241-254.	3.2	9

#	Article	IF	CITATIONS
541	Mechanistic insights into the reversible lithium storage in an open porous carbon via metal cluster formation in all solid-state batteries. Carbon, 2022, 188, 325-335.	10.3	9
542	Zur Struktur und Reaktivit�t des Diammoniumhexafluoromanganats(IV). Zeitschrift Fur Anorganische Und Allgemeine Chemie, 1997, 623, 1259-1263.	1.2	8
543	Synthesis and Structure of the Metallic K6Tl17:Â A Layered Tetrahedral Star Structure Related to That of Cr3Si. Inorganic Chemistry, 2003, 42, 1835-1841.	4.0	8
544	Atmosphericâ€Pressure Plasmas for Solar Cell Manufacturing. Contributions To Plasma Physics, 2009, 49, 662-670.	1.1	8
545	Synthesis of LiNbO <sub>3</sub> nanoparticles in a mesoporous matrix. Beilstein Journal of Nanotechnology, 2011, 2, 28-33.	2.8	8
546	Nanocomposites and Hybrid Materials. , 2012, , 177-209.		8
547	A new molecular silver precursor for the preparation of thin conductive silver films. Journal of Physics and Chemistry of Solids, 2013, 74, 1546-1552.	4.0	8
548	Network Topology. , 0, , 5-40.		8
549	5â€(2â€Mercaptoethyl)â€1 <i>H</i> â€tetrazole: Facile Synthesis and Application for the Preparation of Water Soluble Nanocrystals and Their Gels. Chemistry - A European Journal, 2016, 22, 14746-14752.	3.3	8
550	Theoretical and experimental investigations of <sup>129</sup> Xe NMR chemical shift isotherms in metal–organic frameworks. Physical Chemistry Chemical Physics, 2018, 20, 25039-25043.	2.8	8
551	Molecular Diffusion in a Flexible Mesoporous Metal–Organic Framework over the Course of Structural Contraction. Journal of Physical Chemistry Letters, 2020, 11, 9696-9701.	4.6	8
552	Low Temperature Calorimetry Coupled with Molecular Simulations for an In-Depth Characterization of the Guest-Dependent Compliant Behavior of MOFs. Chemistry of Materials, 2020, 32, 3489-3498.	6.7	8
553	Linker Expansion and Its Impact on Switchability in Pillared-Layer MOFs. Inorganic Chemistry, 2021, 60, 1726-1737.	4.0	8
554	Unraveling the Guestâ€Induced Switchability in the Metalâ€Organic Framework DUTâ€13(Zn)**. Chemistry - A European Journal, 2021, 27, 9708-9715.	3.3	8
555	Nanoporous carbon architectures for iontronics: Ion-based computing, logic circuits and biointerfacing. Chemical Engineering Journal, 2021, 420, 130431.	12.7	8
556	Largeâ€Scale Synthesis of Nanostructured Carbonâ€Ti <sub>4</sub> O <sub>7</sub> Hollow Particles as Efficient Sulfur Host Materials for Multilayer Lithiumâ€Sulfur Pouch Cells. Batteries and Supercaps, 2022, 5, .	4.7	8
557	Synthese und Struktur von Li2Ta2O3F6. Zeitschrift Fur Anorganische Und Allgemeine Chemie, 1997, 623, 456-460.	1.2	7
558	Growth of silica nanoparticles in methylmethacrylate-based water-in-oil microemulsions. Colloid and Polymer Science, 2007, 285, 1645-1653.	2.1	7

#	Article	IF	CITATIONS
559	Ceria/silicon carbide core–shell materials prepared by miniemulsion technique. Beilstein Journal of Nanotechnology, 2011, 2, 638-644.	2.8	7
560	Confocal Microscopy for Process Monitoring and Wide-Area Height Determination of Vertically-Aligned Carbon Nanotube Forests. Coatings, 2015, 5, 477-487.	2.6	7
561	Using neutron powder diffraction and first-principles calculations to understand the working mechanisms of porous coordination polymer sorbents. Acta Crystallographica Section B: Structural Science, Crystal Engineering and Materials, 2015, 71, 648-660.	1.1	7
562	Combination of Zinc Oxide and Antimony Doped Tin Oxide Nanocoatings for Glazing Application. Coatings, 2018, 8, 248.	2.6	7
563	Metal-Organic Frameworks. Green Energy and Technology, 2019, , 137-172.	0.6	7
564	Collective Breathing in an Eightfold Interpenetrated Metal–Organic Framework: From Mechanistic Understanding towards Threshold Sensing Architectures. Angewandte Chemie, 2020, 132, 4521-4527.	2.0	7
565	Solvent-assisted delamination of layered copper dithienothiophene-dicarboxylate (DUT-134). Inorganic Chemistry Frontiers, 2021, 8, 3308-3316.	6.0	7
566	The Role of Metal–Organic Frameworks in Moderating Platinum-Based Ethanol Electrooxidation Catalysts. Journal of Physical Chemistry C, 2021, 125, 14263-14274.	3.1	7
567	Integration of Fluorescent Functionality into Pressure-Amplifying Metal–Organic Frameworks. Chemistry of Materials, 2021, 33, 7964-7971.	6.7	7
568	The Importance of Swelling Effects on Cathode Density and Electrochemical Performance of Lithiumâ^'Sulfur Battery Cathodes Produced via Dry Processing. Energy Technology, 2022, 10, 2100721.	3.8	7
569	Metalâ€Organic Frameworks: Synthesis, Structures, and Applications. Small Structures, 2022, 3, .	12.0	7
570	CdTe nanoparticles for the deposition of CdTe films using close spaced sublimation. Journal of Crystal Growth, 2010, 312, 2449-2453.	1.5	6
571	MOF Shaping and Immobilization. , 2011, , 353-381.		6
572	Atmospheric pressure PECVD based on a linearly extended DC arc for adhesion promotion applications. Surface and Coatings Technology, 2013, 234, 8-13.	4.8	6
573	Pulse plating of platinum on aligned multiwalled carbon nanotubes. Surface Engineering, 2013, 29, 427-433.	2.2	6
574	Functional group tolerance in BTB-based metal–organic frameworks (BTB – benzene-1,3,5-tribenzoate). Microporous and Mesoporous Materials, 2015, 216, 42-50.	4.4	6
575	Electron Paramagnetic Resonance. , 0, , 629-656.		6
576	Alkaline Earth Metal-Based Metal-Organic Frameworks: Synthesis, Properties, and Applications. , 0, , 73-103.		6

#	Article	IF	CITATIONS
577	<i>In Situ</i> Studies of the Crystallization of Metal-Organic Frameworks. , 0, , 729-764.		6
578	Tailoring the Adsorption of ACE-Inhibiting Peptides by Nitrogen Functionalization of Porous Carbons. Langmuir, 2019, 35, 9721-9731.	3.5	6
579	An Asymmetric Supercapacitor–Diode (CAPode) for Unidirectional Energy Storage. Angewandte Chemie, 2019, 131, 13194-13199.	2.0	6
580	Green Precursors and Soft Templating for Printing Porous Carbonâ€Based Microâ€supercapacitors. Chemistry - A European Journal, 2021, 27, 1356-1363.	3.3	6
581	Preparation and Application of ZIF-8 Thin Layers. Applied Sciences (Switzerland), 2021, 11, 4041.	2.5	6
582	Selective Permeable Lithiumâ€lon Channels on Lithium Metal for Practical Lithium–Sulfur Pouch Cells. Angewandte Chemie, 2021, 133, 18179-18184.	2.0	6
583	Surface polarity estimation of metal-organic frameworks using liquid-phase mixture adsorption. Microporous and Mesoporous Materials, 2017, 251, 129-134.	4.4	6
584	Tuning Adsorption-Induced Responsiveness of a Flexible Metal–Organic Framework JUK-8 by Linker Halogenation. Chemistry of Materials, 2022, 34, 3430-3439.	6.7	6
585	Electrochemical Patterning of Cu Current Collectors: An Enabler for Pure Silicon Anodes in Highâ€Energy Lithiumâ€ion Batteries. Advanced Materials Interfaces, 2022, 9, .	3.7	6
586	Synthesis, Structure, and Characterization of [RAl(μ-NHEt)(μ-NEt)2Si(NHEt)]2 (R = Me, Et). European Journal of Inorganic Chemistry, 2003, 2003, 1193-1196.	2.0	5
587	Synthesis of Nanostructured Bismuth Titanate Microspheres. Journal of Nanoscience and Nanotechnology, 2006, 6, 2110-2116.	0.9	5
588	Vertical Aligned Carbon Nanotube Deposition on Metallic Substrates by CVD. ECS Transactions, 2009, 25, 1047-1051.	0.5	5
589	ZnS:Cu Polymer Nanocomposites for Thin Film Electroluminescent Devices. Journal of Nanoscience and Nanotechnology, 2010, 10, 4335-4340.	0.9	5
590	Preparation and microcontact printing of platinum and palladium thin films. Journal of Materials Chemistry C, 2013, 1, 2477.	5.5	5
591	IR and Raman Spectroscopies Probing MOFs Structure, Defectivity, and Reactivity. , 0, , 657-690.		5
592	Solutionâ€Based Chemical Process for Synthesis of Highly Active Li <sub>2</sub> S/Carbon Nanocomposite for Lithium‣ulfur Batteries. ChemNanoMat, 2016, 2, 656-659.	2.8	5
593	Granulation and Shaping of Metal-Organic Frameworks. , 0, , 551-572.		5
594	Synthesis, Structure, and Selected Properties of Aluminum-, Gallium-, and Indium-Based Metal-Organic		5

Frameworks. , 0, , 105-135.

#	Article	IF	CITATIONS
595	Estimating pore size distributions of activated carbons via optical calorimetry. Adsorption, 2017, 23, 313-320.	3.0	5
596	An Innovative Technique for Rapid Screening of Cigarette Filter Adsorbents. Chemical Engineering and Technology, 2017, 40, 71-75.	1.5	5
597	A fast route to obtain modified tin oxide aerogels using hydroxostannate precursors. Materials Chemistry Frontiers, 2018, 2, 710-717.	5.9	5
598	Highly transparent metal electrodes via direct printing processes. Materials Research Bulletin, 2018, 98, 231-234.	5.2	5
599	Platinum Deposited on Carbon Supports for the Complete Detoxification of Formaldehyde at Room Temperature under Humid Conditions. ChemNanoMat, 2018, 4, 1000-1006.	2.8	5
600	Layered α-TiCl <sub>3</sub> : Microsheets on YSZ Substrates for Ethylene Polymerization with Enhanced Activity. Chemistry of Materials, 2019, 31, 5305-5313.	6.7	5
601	Elucidating the Structural Evolution of a Highly Porous Responsive Metal–Organic Framework (DUT-49(M)) upon Guest Desorption by Time-Resolved in Situ Powder X-ray Diffraction. Crystal Growth and Design, 2021, 21, 270-276.	3.0	5
602	Influence of external stack pressure on the performance of Li-S pouch cell. JPhys Energy, 2022, 4, 014004.	5.3	5
603	Mixed-Metal Ni <sup>2+</sup> –Mn <sup>2+</sup> Paddle Wheels in the Metal–Organic Framework DUT-8(Ni <sub>1–<i>x</i></sub> Mn <sub><i>x</i></sub> ) as Electron Paramagnetic Resonance Probes for Monitoring the Structural Phase Transition. Journal of Physical Chemistry C, 2022, 126, 625-633.	3.1	5
604	Surface Functionalization of LiNi <sub>7.0</sub> Co <sub>0.15</sub> Mn <sub>0.15</sub> O <sub>2</sub> with Fumed Li <sub>2</sub> ZrO <sub>3</sub> via a Costâ€Effective Dryâ€Coating Process for Enhanced Performance in Solidâ€Etate Batteries. Batteries and Supercaps, 2022, 5, .	4.7	5
605	Solid-state NMR studies of metal ion and solvent influences upon the flexible metal-organic framework DUT-8. Solid State Nuclear Magnetic Resonance, 2022, 120, 101809.	2.3	5
606	Opening and Reversible Filling of Single-Walled Carbon Nanotubes with Various Materials. Journal of Nanoscience and Nanotechnology, 2006, 6, 3360-3363.	0.9	4
607	Characterization of the microporosity of different metal-organic frameworks using 129Xe NMR spectroscopy. Studies in Surface Science and Catalysis, 2007, , 2030-2036.	1.5	4
608	Effect of synthesis conditions on porous structure, luminescence and absorption properties of dye-loaded silica xerogels. Microporous and Mesoporous Materials, 2011, 142, 245-250.	4.4	4
609	Rapid and scalable method for direct and indirect microstructuring of vertical aligned carbon nanotubes. Surface and Coatings Technology, 2012, 206, 4808-4813.	4.8	4
610	Transparent thin films of Bi2WO6, Bi4Ti3O12 and Sr0.75Ba0.25Nb2O6. Solid State Sciences, 2012, 14, 1378-1384.	3.2	4
611	Fabrication of Nanoparticle-Containing Films and Nano Layers for Alloying and Joining. Advanced Engineering Materials, 2014, 16, 1264-1269.	3.5	4
612	K <sub>2</sub> S <sub>6</sub> , a Potassium Polysulfide with Long Sulfur Chain. Zeitschrift Fur Anorganische Und Allgemeine Chemie, 2014, 640, 905-906.	1.2	4

#	Article	IF	CITATIONS
613	Reticular Chemistry of Metal-Organic Frameworks Composed of Copper and Zinc Metal Oxide Secondary Building Units as Nodes. , 0, , 41-72.		4
614	Molecular Precursors for Tailoring Humidity Tolerance of Nanoscale Hopcalite Catalysts Via Flame Spray Pyrolysis. ChemCatChem, 2019, 11, 4593-4603.	3.7	4
615	Conductive ITO Interfaces for Optoelectronic Applications Based on Highly Ordered Inverse Opal Thin Films. ChemNanoMat, 2020, 6, 560-566.	2.8	4
616	NMR analysis of phosphoric acid distribution in porous fuel cell catalysts. Chemical Communications, 2021, 57, 2547-2550.	4.1	4
617	Energetic carbon precursors for micro-supercapacitor printing. Materials Advances, 2021, 2, 6380-6387.	5.4	4
618	Characterisation of Porous Solids VIII. Special Publication - Royal Society of Chemistry, 2009, , .	0.0	4
619	Parameter optimization of light outcoupling structures for high-efficiency organic light-emitting diodes. Journal of Applied Physics, 2020, 128, 185501.	2.5	4
620	Ordered mesoporous silicon carbide. Studies in Surface Science and Catalysis, 2007, , 1770-1773.	1.5	3
621	Highly Transparent Bi <sub>2</sub> MoO <sub>6</sub> - and Bi <sub>2</sub> WO <sub>6</sub> -Polymer Nanocomposites. Journal of Nanoscience and Nanotechnology, 2011, 11, 3464-3469.	0.9	3
622	Chiral Linker Systems. , 0, , 387-419.		3
623	Porous Metal Azolate Frameworks. , 2016, , 309-343.		3
624	Defects and Disorder in MOFs. , 2016, , 795-822.		3
625	A novel approach to rapid sizing of nanoparticles by using optical calorimetry. Advanced Powder Technology, 2017, 28, 1065-1068.	4.1	3
626	Extended DC arc atmospheric pressure plasma source for large scale surface cleaning and functionalization. Contributions To Plasma Physics, 2018, 58, 327-336.	1.1	3
627	Lithium–Sulfur Batteries. Energy Technology, 2019, 7, 1900940.	3.8	3
628	A bifunctional metal–organic framework platform for catalytic applications. Polyhedron, 2019, 159, 382-386.	2.2	3
629	First example of Ugi's amine as a platform for the construction of chiral coordination polymers: synthesis and properties. New Journal of Chemistry, 2021, 45, 2791-2794.	2.8	3
630	Monolithic Inâ€Plane Integration of Gateâ€Modulated Switchable Supercapacitors. Energy Technology, 2022, 10, .	3.8	3

#	Article	IF	CITATIONS
631	Iron and Groups V- and VI-based MOFs. , 0, , 171-202.		2
632	Nanoparticles. , 0, , 491-521.		2
633	New solar selective coating based on carbon nanotubes. AIP Conference Proceedings, 2016, , .	0.4	2
634	<i>In Situ</i> X-ray Diffraction and XAS Methods. , 0, , 691-727.		2
635	Group 4 Metals as Secondary Building Units: Ti, Zr, and Hf-based MOFs. , 2016, , 137-170.		2
636	Rapid Screening of CO Oxidation Catalysts Using Optical Calorimetry. Industrial & Engineering Chemistry Research, 2019, 58, 19839-19846.	3.7	2
637	Dynamic Metalâ€Organic Frameworks: Unraveling Structure and Dynamics in Porous Frameworks via Advanced In Situ Characterization Techniques (Adv. Funct. Mater. 41/2020). Advanced Functional Materials, 2020, 30, 2070272.	14.9	2
638	Synthesis and Structure of the Silver(I) Complexes [Ag <sub>2</sub> (C <sub>4</sub> H <sub>6</sub> O <sub>4</sub> N)NO <sub>3</sub> ]·H <sub>2</sub> O and Ag <sub>6</sub> (C <sub>6</sub> H <sub>6</sub> O <sub>6</sub> N) <sub>2</sub> for the Formulation of Silver Inks in Nanoimprint Lithography. European Journal of Inorganic Chemistry,	2.0	2
639	2020, 2020, 3167-3173. Highâ€Performing Liâ€Ion Battery with "Two Cathodes in One―of Sulfur and LiFePO 4 by Strategies of Mitigation of Polysulfide Shuttling. Batteries and Supercaps, 2021, 4, 359-367.	4.7	2
640	A new zeolitic lithium aluminum imidazolate framework. Dalton Transactions, 2021, 50, 7933-7937.	3.3	2
641	Advanced characterisation techniques: multi-scale, <i>in situ</i> , and time-resolved: general discussion. Faraday Discussions, 2021, 225, 152-167.	3.2	2
642	Lithium Metal Anode: Processing and Interface Engineering. Batteries and Supercaps, 2021, 4, 690-691.	4.7	2
643	Massive Pressure Amplification by Stimulated Contraction of Mesoporous Frameworks**. Angewandte Chemie, 2021, 133, 11841-11845.	2.0	2
644	Increasing the Stability of LiMn <sub>2</sub> O <sub>4</sub> Against Harsh Conditions During Lithium Recovery from Real Brine Solutions. Energy Technology, 2021, 9, 2100145.	3.8	2
645	Solid-state NMR insights into alcohol adsorption by metal–organic frameworks: adsorption state, selectivity, and adsorption-induced phase transitions. Chemical Communications, 2022, 58, 4492-4495.	4.1	2
646	Cooperative Assembly of 2Dâ€MOF Nanoplatelets into Hierarchical Carpets and Tubular Superstructures for Advanced Air Filtration. Angewandte Chemie - International Edition, 2022, , .	13.8	2
647	The effect of cationic disordering on the electrochemical performances of the layered nitrides LiWN2 and Li0.84W1.16N2. Journal of the European Ceramic Society, 2007, 27, 4199-4203.	5.7	1
648	Metalâ€Organic Frameworks as Gas Storage Materials. Zeitschrift Fur Anorganische Und Allgemeine Chemie, 2008, 634, 2023-2023.	1.2	1

#	Article	IF	CITATIONS
649	MEMS analyzer for fast determination of mixed gases. , 2009, , .		1
650	Transparent magnesium hydroxide/acrylate nanocomposite films. Journal of Applied Polymer Science, 2010, 116, 2197-2204.	2.6	1
651	Investigation on atmospheric plasma surface treatment for structural bonding on titanium and CFRP. , 2015, , .		1
652	Transparente und leitfÄ <b>¤</b> ige Veredelung von KunststoffoberflÄ <b>ë</b> hen. Vakuum in Forschung Und Praxis, 2015, 27, 36-40.	0.1	1
653	Extended Linkers for Ultrahigh Surface Area Metal-Organic Frameworks. , 2016, , 271-307.		1
654	Functional Linkers for Electron-Conducting MOFs. , 0, , 421-462.		1
655	Nuclear Magnetic Resonance of Metal-Organic Frameworks (MOFs). , 2016, , 607-628.		1
656	Linkers with Optical Functionality. , 2016, , 463-489.		1
657	Functional Linkers for Catalysis. , 2016, , 345-386.		1
658	Role of Molecular Simulations in the Field of MOFs. , 2016, , 765-794.		1
659	SURMOFs: Liquid-Phase Epitaxy of Metal-Organic Frameworks on Surfaces. , 2016, , 523-550.		1
660	Group 3 Elements and Lanthanide Metals. , 0, , 231-270.		1
661	Adsorption Methodology. , 0, , 575-605.		1
662	Investigations on clean and efficient remote cutting and ablating processes. Procedia CIRP, 2018, 74, 413-416.	1.9	1
663	Natural Polymer-Based MOF Composites. , 2021, , 321-348.		1
664	Novel computational tools: general discussion. Faraday Discussions, 2021, 225, 341-357.	3.2	1
665	<i>Batteries &amp; Supercaps</i> : In Situ and Operando Methods for Energy Storage and Conversion. Batteries and Supercaps, 2021, 4, 1789-1790.	4.7	1
666	Pore-Size Engineering of Silicon Imido Nitride for Catalytic Applications. Angewandte Chemie - International Edition, 2001, 40, 4204-4207.	13.8	1

#	Article	IF	CITATIONS
667	Cooperative Assembly of 2Dâ€MOF Nanoplatelets into Hierarchical Carpets and Tubular Superstructures for Advanced Air Filtration. Angewandte Chemie, 2022, 134, .	2.0	1
668	Template Assisted Design of Microporous Gallium Nitride Materials ChemInform, 2003, 34, no.	0.0	0
669	Synthesis and Structure of the Metallic K6Tl17: A Layered Tetrahedral Star Structure Related to that of Cr3Si ChemInform, 2003, 34, no.	0.0	Ο
670	Improved Hydrogen Storage Properties of Ti-Doped Sodium Alanate Using Titanium Nanoparticles as Doping Agents ChemInform, 2003, 34, no.	0.0	0
671	Porous Metal-Organic Frameworks. ChemInform, 2004, 35, no.	0.0	0
672	Syntheses and Catalytic Properties of Titanium Nitride Nanoparticles. , 0, , 279-293.		0
673	Metal-Organic Frameworks. Zeitschrift Fur Anorganische Und Allgemeine Chemie, 2006, 632, 2090-2090.	1.2	Ο
674	Synthese und katalytische Eigenschaften von CeO <sub>2</sub> Nanopartikeln aus inversen Mikroemulsionen. Zeitschrift Fur Anorganische Und Allgemeine Chemie, 2008, 634, 2078-2078.	1.2	0
675	Magnetic Resonance and Local Properties of BiFeO <sub>3</sub> and Ni <sub>2</sub> MnGa Layers. Ferroelectrics, 2008, 370, 153-155.	0.6	Ο
676	Synthesis and catalytic application of ceria nanoparticles and ceria-SiC composites. Materials Research Society Symposia Proceedings, 2009, 1217, 1.	0.1	0
677	Inorganic Porous MaterialsÂ. Zeitschrift Fur Anorganische Und Allgemeine Chemie, 2010, 636, 2037-2037.	1.2	Ο
678	Mesoporous ZriVand HfiVmetal–organic frameworks with reo topology. Acta Crystallographica Section A: Foundations and Advances, 2012, 68, s225-s225.	0.3	0
679	Tracking the Changes in Active Carbon Pore Structure during Physical Activation Using the Thermal Response Screening Method. Chemie-Ingenieur-Technik, 2013, 85, 1363-1364.	0.8	Ο
680	Batteries: Carbon-Based Anodes for Lithium Sulfur Full Cells with High Cycle Stability (Adv. Funct.) Tj ETQq0 0 0	rgBT /Ove 14.9	rlock 10 Tf 50
681	D2 Enertrode: Production Technologies and Component Integration of Nanostructured Carbon Electrodes for Energy Technology—Functionalized Carbon Materials for Efficient Electrical Energy Supply. Advanced Engineering Materials, 2014, 16, 1196-1201.	3.5	Ο
682	Appendix A: MOF Suppliers. , 0, , 823-823.		0
683	Appendix B: Datasheets. , 2016, , 825-832.		Ο

684 Platinum Group Metal-Organic Frameworks. , 0, , 203-230.

0

#	Article	IF	CITATIONS
685	Innenrücktitelbild: Ultrastable Surfaceâ€Dominated Pseudocapacitive Potassium Storage Enabled by Edgeâ€Enriched Nâ€Đoped Porous Carbon Nanosheets (Angew. Chem. 44/2020). Angewandte Chemie, 2020, 132, 19891-19891.	2.0	0
686	Metal-Organic Frameworks for Environmental Applications. Engineering Materials, 2021, , 1-39.	0.6	0
687	Untersuchung von Dynamik, Struktur und Magnetismus von schaltbaren Metallâ€organischen Gerüstverbindungen mittels 1 Hâ€detektierter MASâ€NMRâ€5pektroskopie. Angewandte Chemie, 2021, 133, 21946-21952.	2.0	0
688	Materials breaking the rules: general discussion. Faraday Discussions, 2021, 225, 255-270.	3.2	0
689	Mechanical Reinforcement of Copper Films with Ceramic Nanoparticles. Ceramic Engineering and Science Proceedings, 0, , 359-366.	0.1	0
690	Plasma Enhanced Chemical Vapour Deposition (PECVD) at Atmospheric Pressure (AP) of Organosilicon Films for Adhesion Promotion on Ti15V3Cr3Sn3Al and Ti6Al4V. Journal of Materials Science and Engineering A, 2015, 5, .	0.1	0
691	Influence of Polysulfides on the Lithium Metal Anode and on Electrolyte Properties. ECS Meeting Abstracts, 2021, MA2021-02, 88-88.	0.0	0
692	Identification of Soluble Degradation Products in Lithium–Sulfur and Lithium-Metal Sulfide Batteries. Separations, 2022, 9, 57.	2.4	0
693	Metal–Organic Frameworks: Special Collection 2020. Chemistry - A European Journal, 2022, 28, e202200607.	3.3	0